SUPPLEMENTARY INFORMATION FOR:

Iron (II) complexes with diazinyl-NHC ligands: Impact of π-deficiency of the azine core on photophysical properties

Mohamed Darari,[a] Edoardo Domenichini,[b] Antonio Francés-Monerris,[c] Cristina Cebrian,[d] Kevin Magra,[d] Marc Beley, [a] Mariachiara Pastore,[c] Antonio Monari,[c] Xavier Assfeld,[c] Stefan Haacke[b] and Philippe C. Gros*[,a]

[a]Université de Lorraine, CNRS, L2CM, F-54000 Nancy, France
[b]Université de Strasbourg, CNRS, IPCMS, F-67000 Strasbourg, France
[c]Université de Lorraine, CNRS, LPCT, F-54000 Nancy, France
[d]Université de Lorraine, CNRS, L2CM, F-57000 Metz, France

Table of contents

NMR Spectra

NMR Spectra of ligands

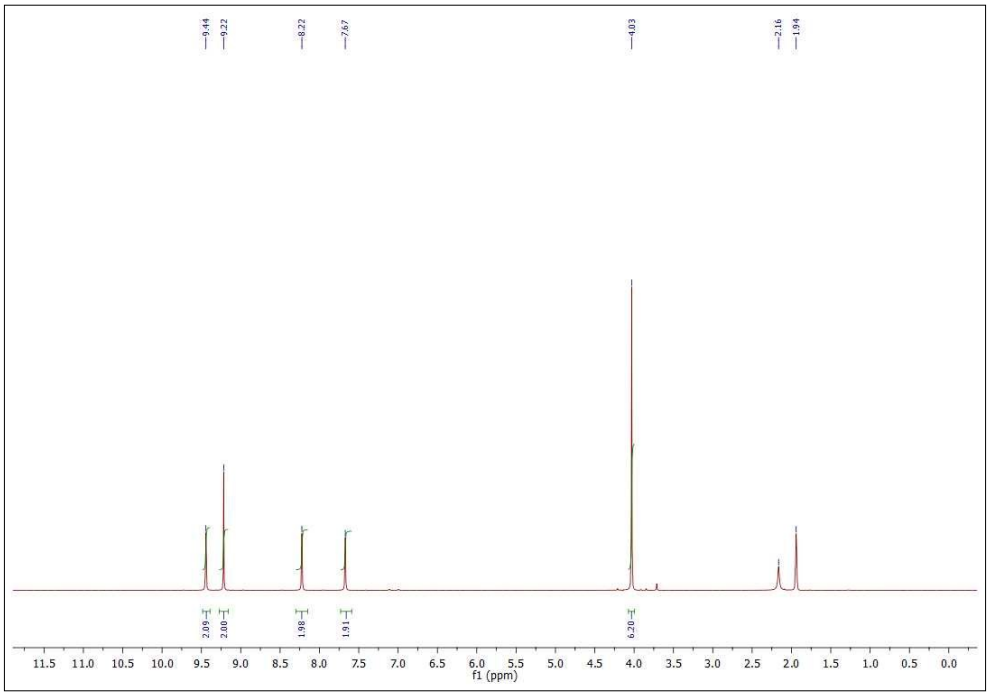

Figure S1 : 1HNMR of L1

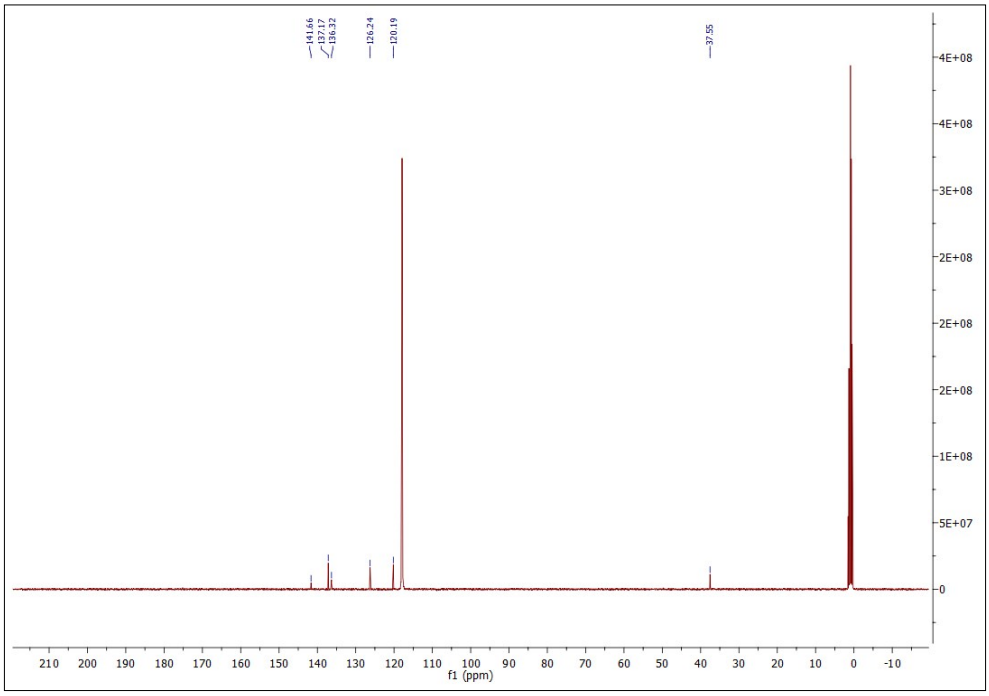

Figure S2 : ^{13}C NMR of L1

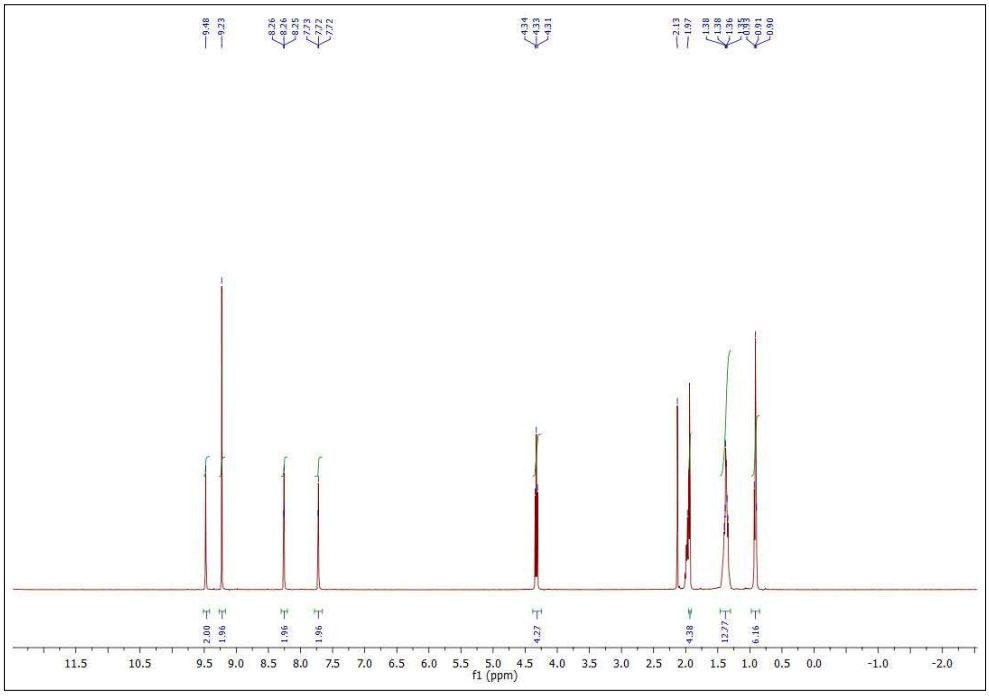

Figure S3 : ^{1}HNMR of L2

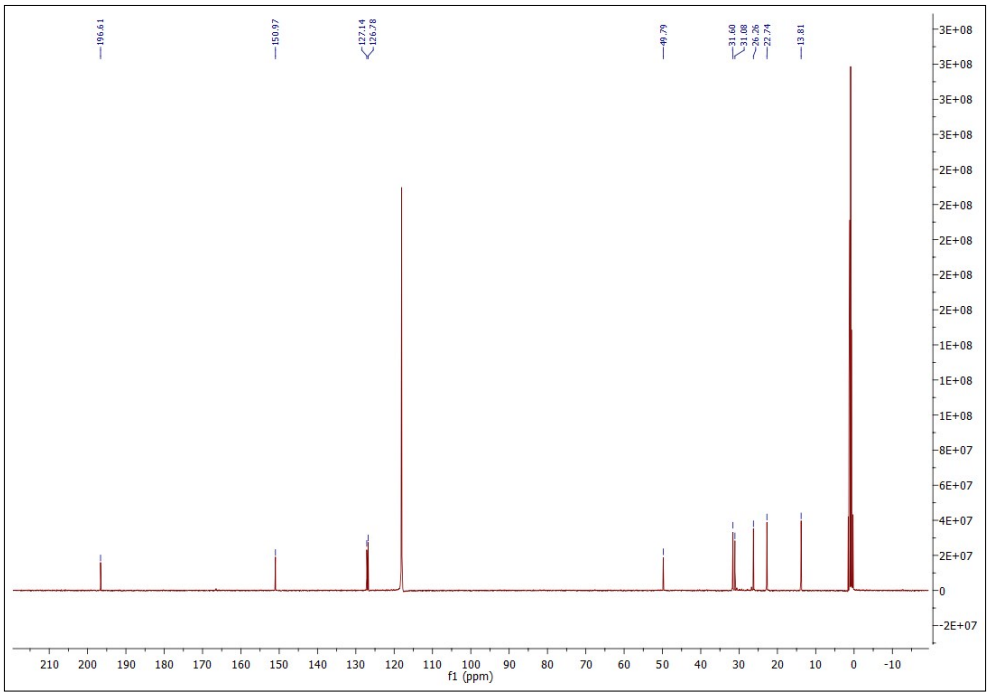

Figure S4 : ^{13}C NMR of L2

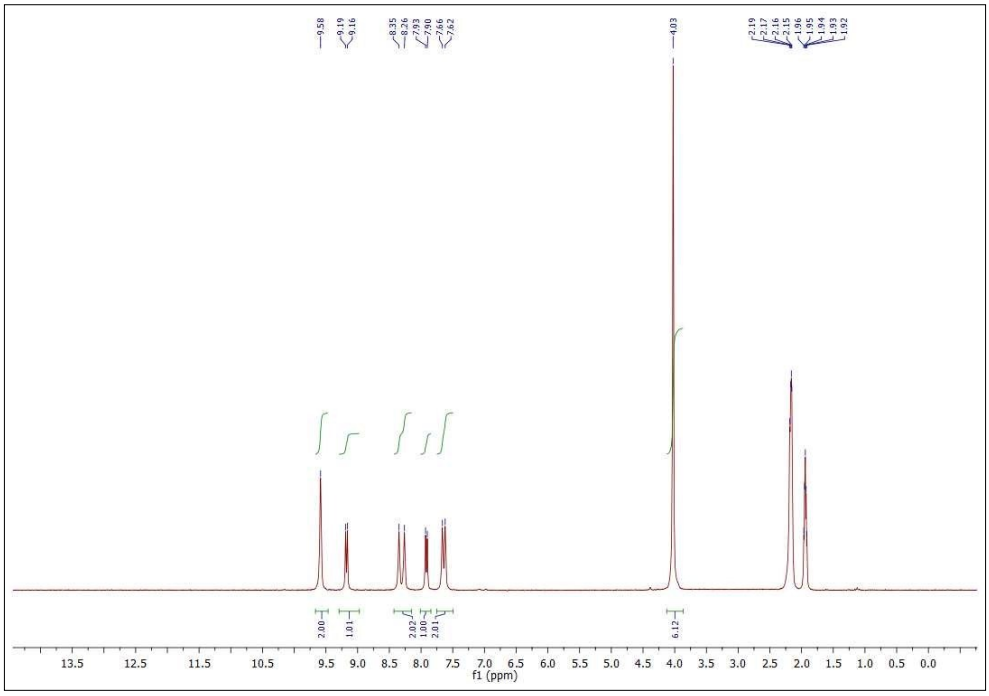

Figure S5 : : ^{1}HNMR of L3

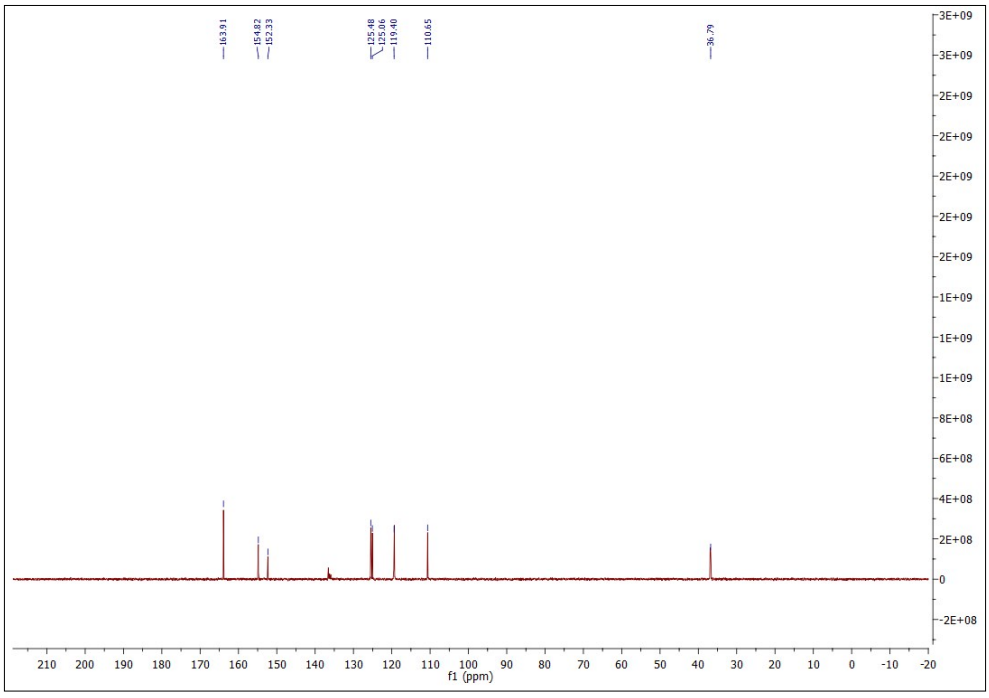

Figure S6 : ^{13}C NMR L3

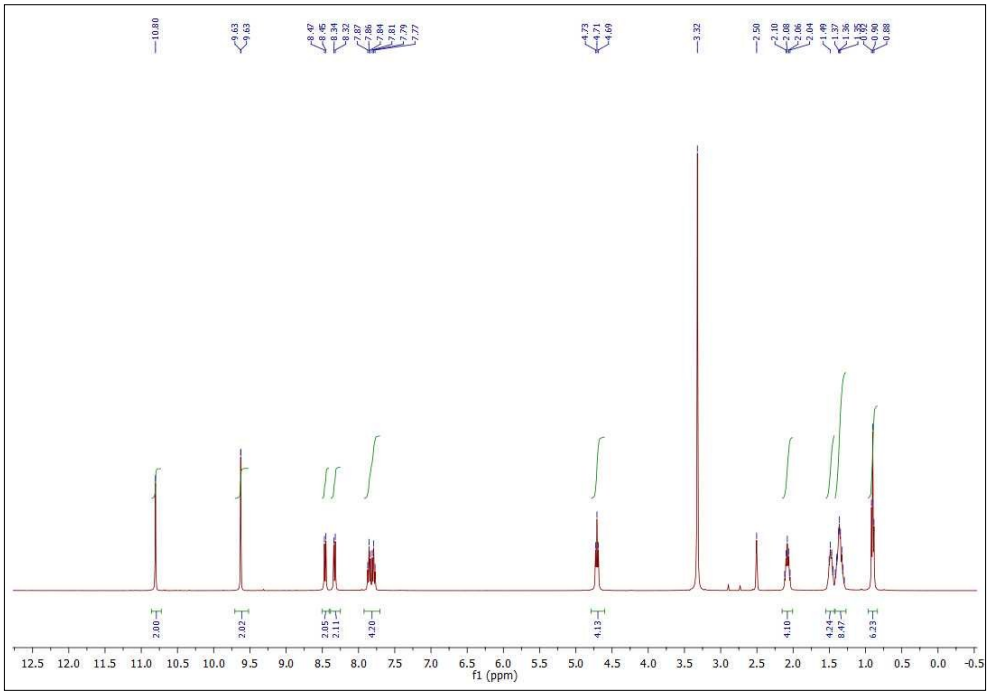

Figure S7 : ^{1}HNMR of L5.Br

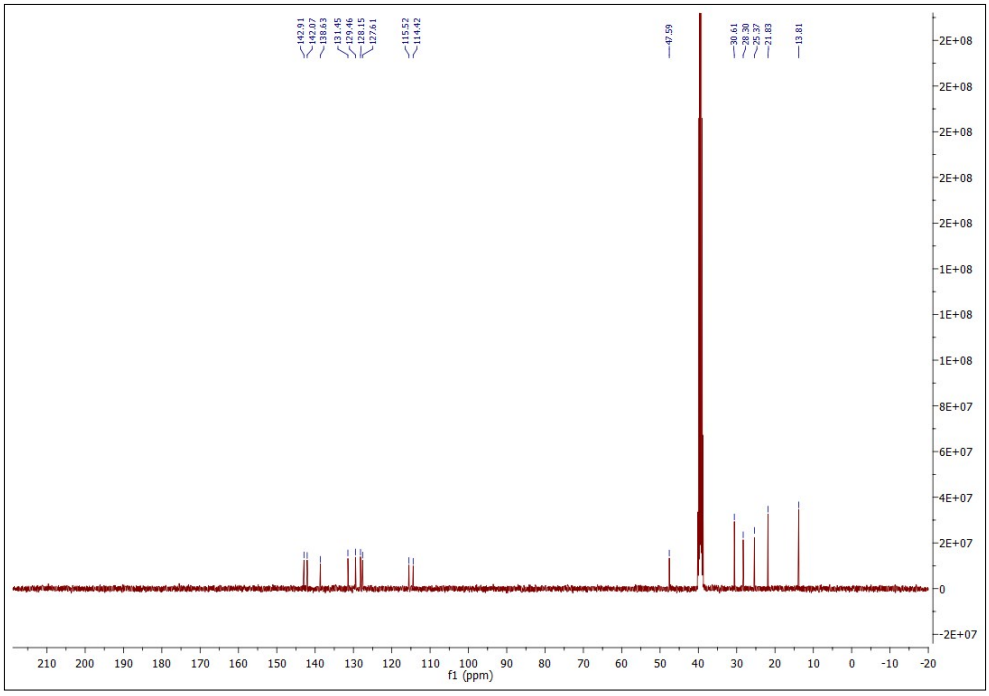

Figure S8 : ^{13}C NMR of L5.Br

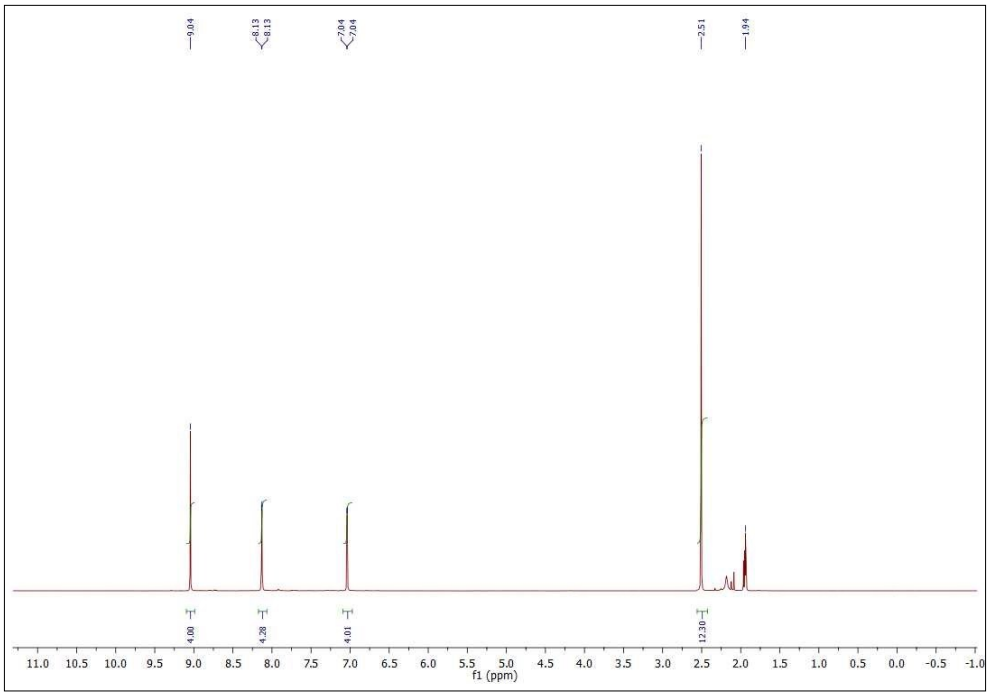

Figure S9 : ^{1}HNMR of C1

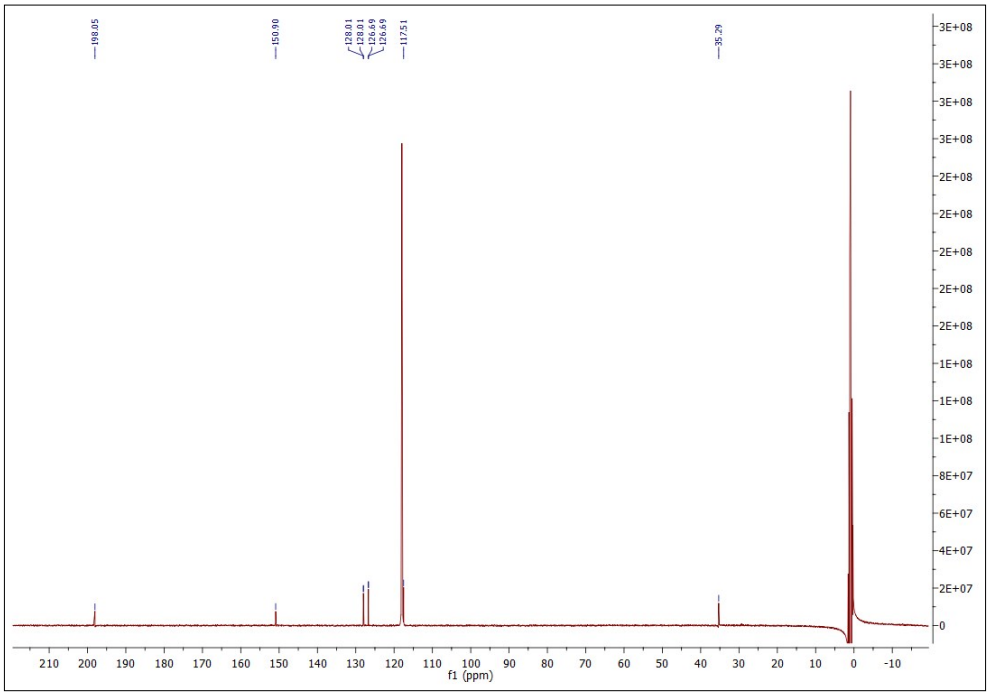

Figure S10 : ^{13}C NMR of C1

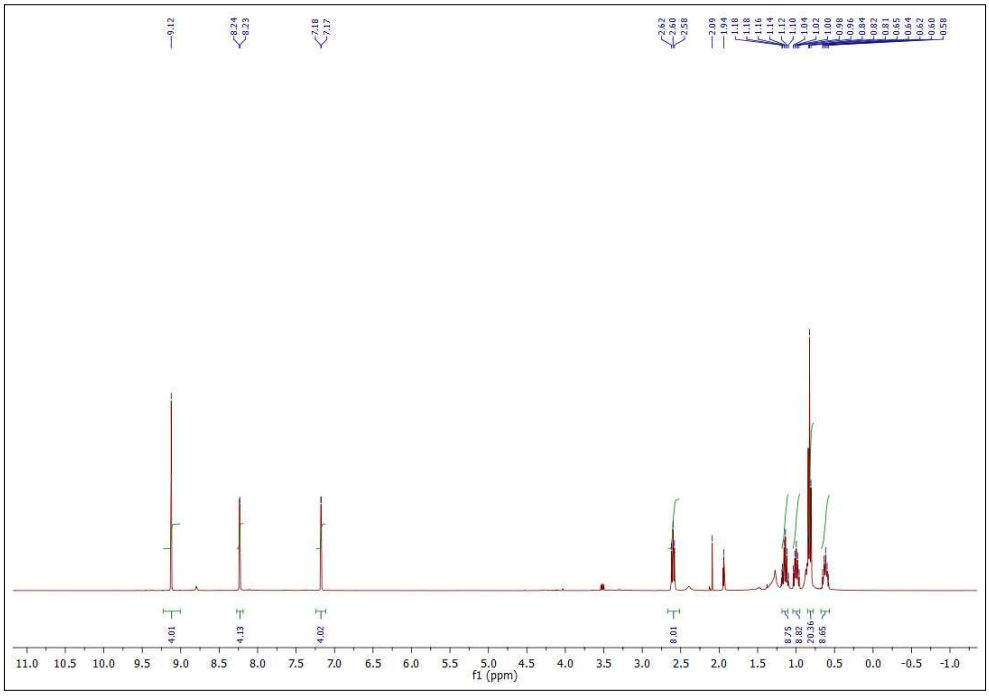

Figure S11 : ^{1}HNMR of C2

Figure S12 : ^{13}C NMR of C2

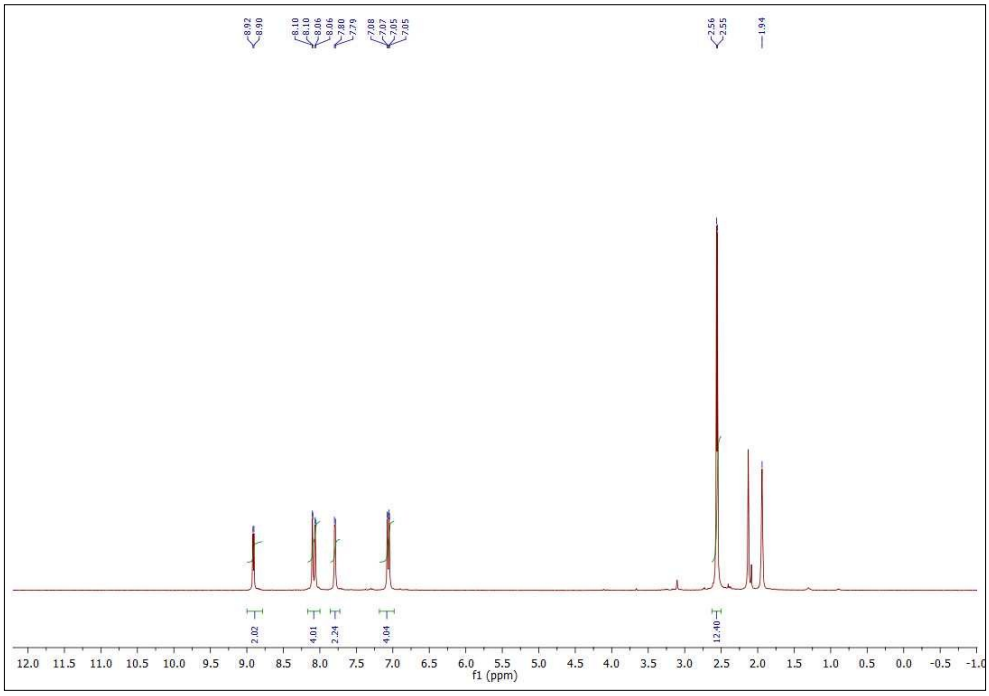

Figure S13 : ^{1}HNMR of C3

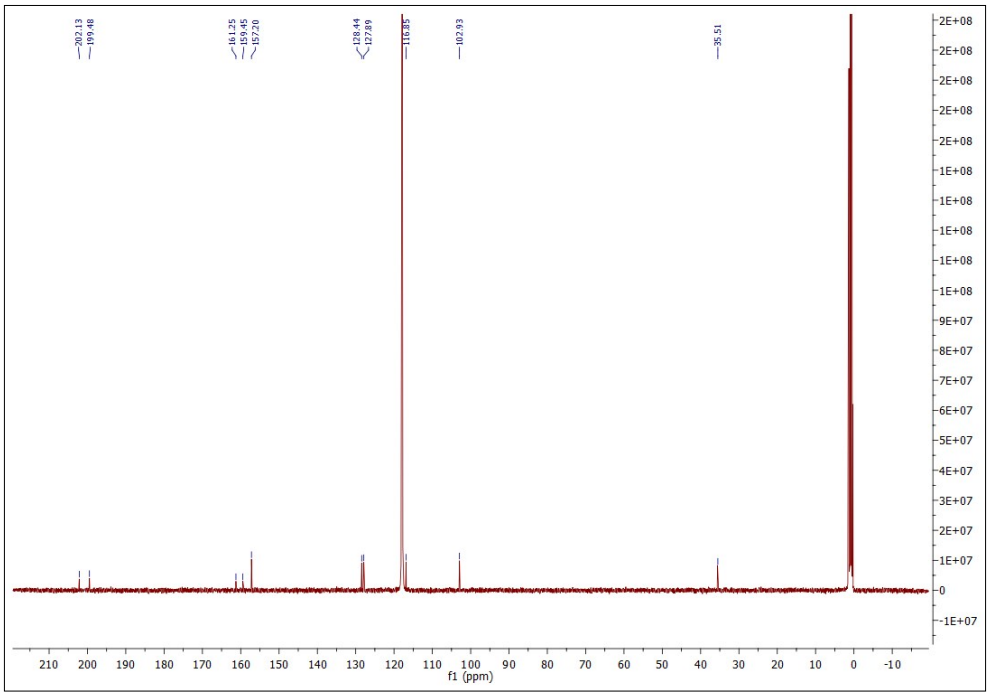

Figure S14 : ^{13}C NMR C3

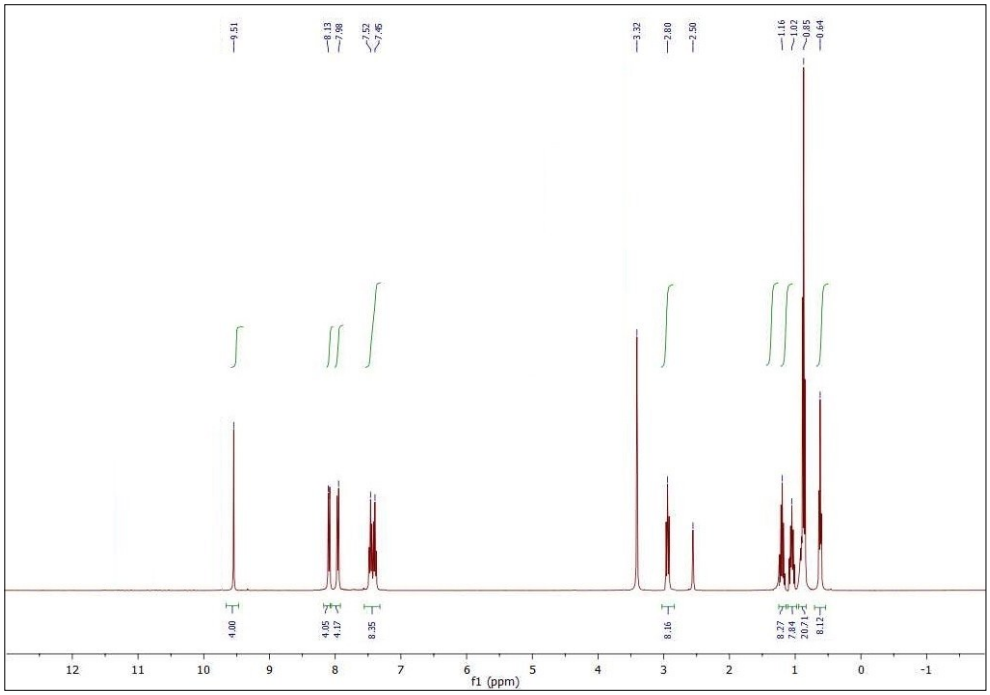

Figure S15 : : ^{1}HNMR of C4

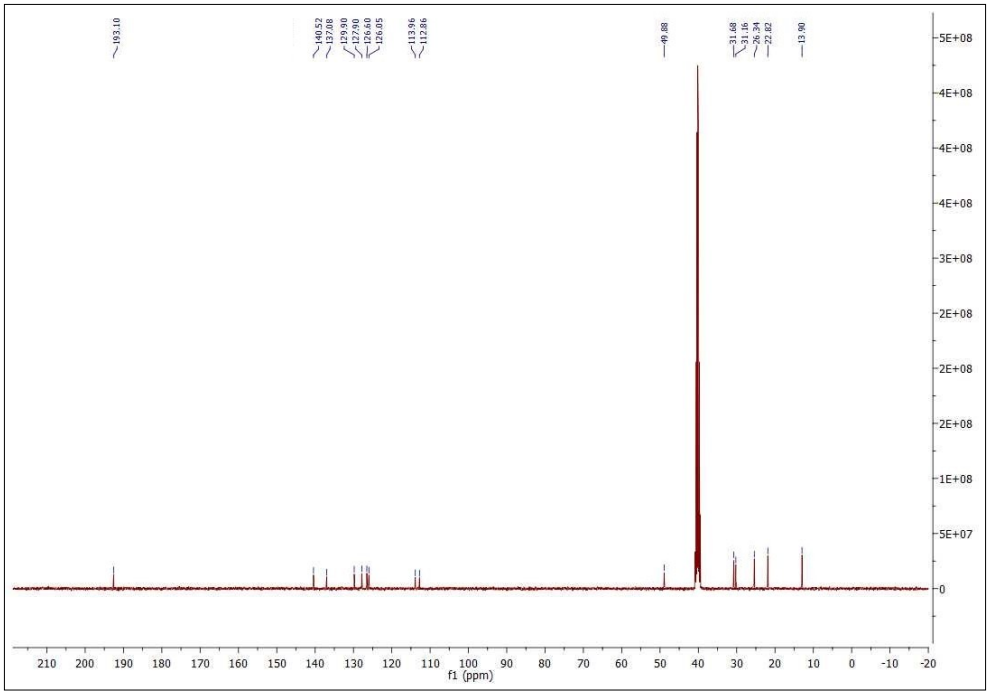

Figure S16 : ^{13}C NMR C4

Computational data

Computed UV-Vis spectrum of complexes C1-C4

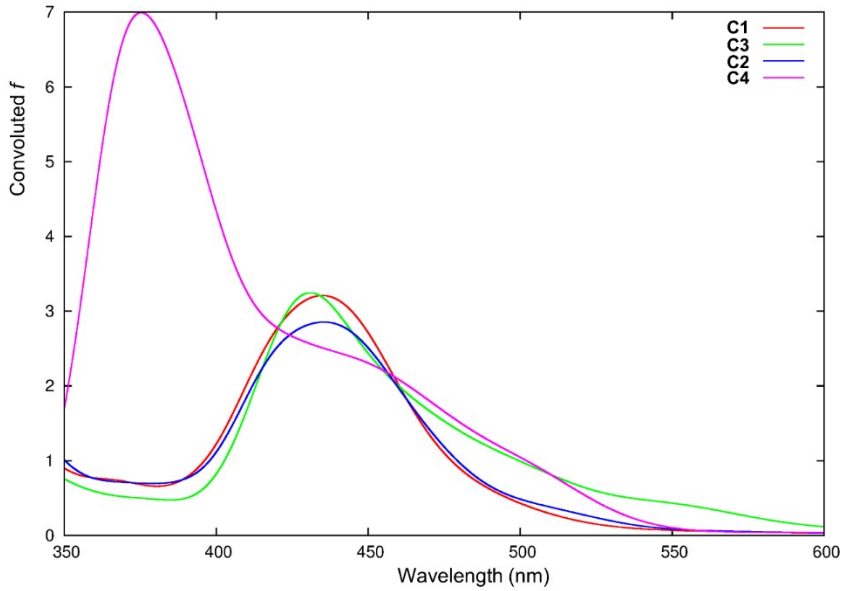

Figure S17. UV-vis absorption spectra obtained with the TD-DFT method.

Natural transition orbitals

Complex	State	oNTO		vNTO	Weight (%)
C1	S_{11} λ = 423 nm (*f* = 0.328)	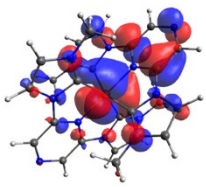	MLCT	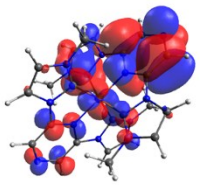	39
C1	S_{11} λ = 423 nm (*f* = 0.328)	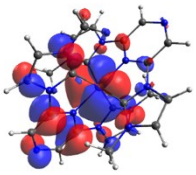	MLCT	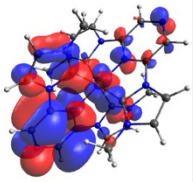	38
C3	S_{11} λ = 423 nm (*f* = 0.328)	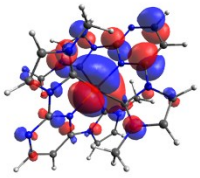	MLCT	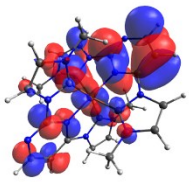	39
C3	S_{11} λ = 423 nm (*f* = 0.328)	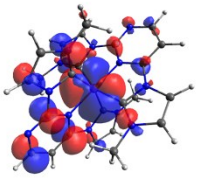	MLCT	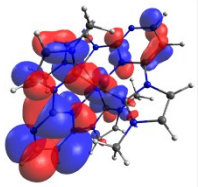	38

Figure S18. Occupied (oNTO) and virtual (vNTO) NTOs of the bright states responsible of the MLCT absorption in the visible range of complexes **C1** and **C3**.

Complex	State	oNTO	vNTO	Weight (%)
C2	S_{11} λ = 427 nm (f = 0.371)	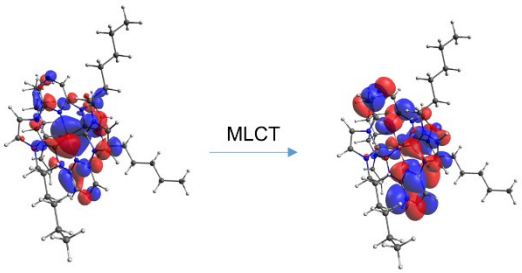		43
C2	S_{11} λ = 427 nm (f = 0.371)	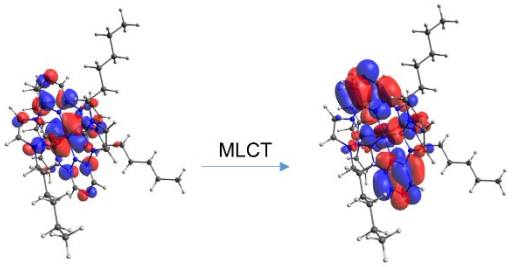		37

Figure S19. Occupied (oNTO) and virtual (vNTO) NTOs of the bright states responsible of the MLCT absorption in the visible range of complex **C2**.

Complex	State	oNTO		vNTO	Weight (%)
C4	S_9 λ = 423 nm (*f* = 0.104)	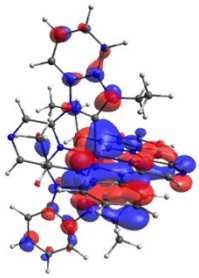	MLCT	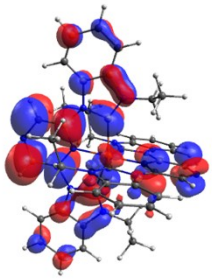	52
C4	S_9 λ = 423 nm (*f* = 0.104)	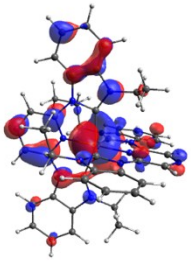	MLCT	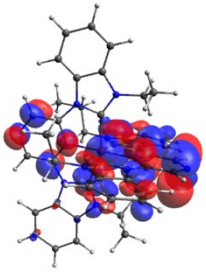	39
C4	S_{29} λ = 369 nm (*f* = 0.306)	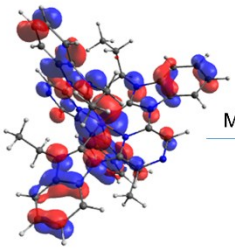	MLCT	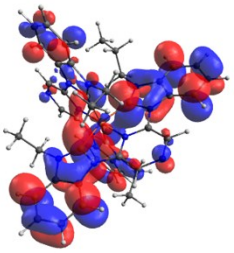	51
C4	S_{29} λ = 369 nm (*f* = 0.306)	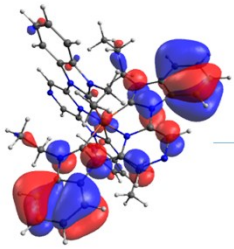	IL	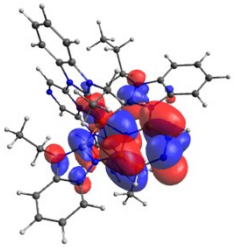	24

Figure S20. Occupied (oNTO) and virtual (vNTO) NTOs of the bright states responsible of the MLCT absorption in the visible range of complex **C4**.

Potential energy surface of C3

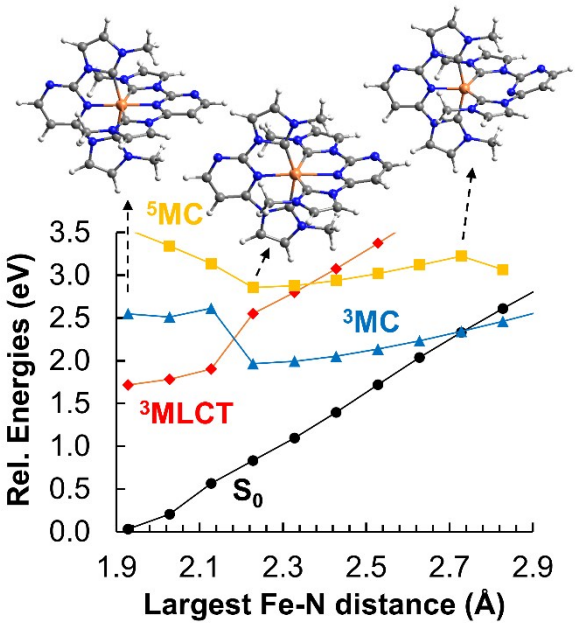

Figure S21. S_0, ^{3}MLCT, ^{3}MC and ^{5}MC potential energy surfaces of **C3** along the Fe-N bond stretch. Relaxed scan calculations on the T_1 surface have been performed at the unrestricted DFT/HCTH/6-31+G(d,p) level of theory, whereas the final energies have been corrected with the TD-HCTH/6-311G(d,p) method.

Cartesian Coordinates

C1 complex

S_0 min (B3LYP/6-31+G(d,p)

Fe	0.139181	0.104414	-0.084645
C	-0.384537	1.397826	-2.575676
C	-1.171454	1.971979	-3.576380
N	-0.946240	0.915899	-1.456051
N	-2.499966	2.051069	-3.429104
C	-2.278631	0.995268	-1.315526
C	-3.066165	1.572296	-2.314001
N	0.996320	1.232376	-2.543974
C	1.531202	0.627281	-1.413354
C	1.983250	1.578092	-3.466369
N	2.857795	0.615613	-1.663032
C	3.151062	1.184728	-2.906569
N	-2.678420	0.441476	-0.103035
C	-3.940002	0.316167	0.477825
C	-1.679986	-0.086847	0.706189
C	-3.728918	-0.298353	1.665200
N	-2.356015	-0.536698	1.784594
C	-1.749195	-1.164691	2.961013
C	3.880010	0.048692	-0.780316
C	1.724911	-0.002029	2.288346
C	2.529671	-0.598679	3.261153
N	1.231684	-0.724814	1.270835
N	2.817271	-1.904663	3.191986
C	1.524137	-2.033059	1.206615

C	2.326729	-2.631542	2.180365
N	1.322172	1.325998	2.189135
C	0.533962	1.666953	1.095527
C	1.561717	2.419660	3.020213
N	0.307222	2.985754	1.274421
C	0.918532	3.459234	2.440049
N	0.930155	-2.615799	0.091474
C	0.950892	-3.928073	-0.379658
C	0.168388	-1.784897	-0.720532
C	0.191297	-3.919351	-1.499798
N	-0.276826	-2.614966	-1.687915
C	-1.116639	-2.220584	-2.821598
C	-0.522872	3.832387	0.415066
H	-0.738826	2.365632	-4.489137
H	-4.143564	1.648803	-2.220646
H	1.774930	2.062312	-4.406136
H	4.162172	1.260563	-3.273665
H	-4.847123	0.661311	0.010035
H	-4.426166	-0.589564	2.434496
H	-1.189054	-0.426775	3.538455
H	-2.543864	-1.573760	3.583856
H	-1.091164	-1.976697	2.653332
H	4.854028	0.429227	-1.086138
H	3.689958	0.355014	0.247005
H	3.882646	-1.041100	-0.850688
H	2.942952	-0.033531	4.088881
H	2.574969	-3.686391	2.148424
H	2.152375	2.365100	3.919580
H	0.842867	4.491271	2.743826
H	1.482547	-4.727565	0.109169
H	-0.063305	-4.719240	-2.176712
H	-0.529628	-1.665975	-3.556537
H	-1.514202	-3.120524	-3.289348
H	-1.948545	-1.611439	-2.470995
H	-0.177530	4.862989	0.497776
H	-0.423460	3.510653	-0.618656
H	-1.569604	3.775472	0.723150

$S_0/^3$MC singlet-triplet crossing (TD-HCTH/6-31G*)

C	-4.283662	-1.073551	0.877748
C	-2.904038	-0.847509	0.905791
N	-2.288535	-0.232603	-0.123526
C	-3.041089	0.154646	-1.173542
C	-4.407572	-0.073955	-1.192799
N	-5.019316	-0.688398	-0.163221
N	-1.974747	-1.163081	1.871317
N	-2.235841	0.770753	-2.135345
C	-2.094810	-1.788533	3.100711
C	-0.840109	-1.824145	3.608050
N	0.015867	-1.228787	2.693786
C	-0.881284	0.872300	-1.859252
N	-0.389768	1.504522	-2.953703
C	-1.385816	1.781361	-3.868023
C	-0.652795	-0.799863	1.591677
C	1.444362	-1.093916	2.920150
C	-2.558499	1.319572	-3.356418
C	1.007334	1.857711	-3.166694
H	-4.793852	-1.569167	1.700388
Fe	-0.399007	0.082417	-0.112091
H	-5.029022	0.230428	-2.030668
H	-3.032796	-2.143979	3.498307
H	-0.482062	-2.224086	4.545288
H	-1.184574	2.281913	-4.803665
H	1.693915	-1.561408	3.872841
H	2.001395	-1.596270	2.127032
H	1.724625	-0.039038	2.961978
H	-3.560320	1.342239	-3.756982
H	1.355910	2.499619	-2.356745
H	1.618967	0.954892	-3.207586
H	1.089446	2.392944	-4.112423

N	2.280556	0.610032	-0.301324
C	2.666137	1.564632	0.508865
H	5.012833	-1.310173	-0.239454
C	2.999814	-0.467129	-0.498084
N	2.201111	-1.510265	-1.003070
C	3.997037	1.580911	0.950567
H	4.408233	2.360883	1.587158
N	4.812739	0.576937	0.604616
N	1.568586	2.351538	0.904723
C	4.335618	-0.476012	-0.071436
H	2.506391	4.169399	1.623958
C	0.269119	1.842936	0.822203
C	1.596155	3.606408	1.484730
C	0.309076	3.914806	1.766042
C	-1.917016	2.821875	1.532299
H	-2.219781	1.929682	2.081877
H	-2.413875	2.847352	0.559639
H	-2.214081	3.702413	2.102128
H	-0.119123	4.801373	2.209745
N	-0.469724	2.841133	1.366675
H	1.383681	-4.372887	-2.302778
C	0.815793	-1.490450	-0.819529
C	2.625045	-2.676260	-1.612832
N	0.435078	-2.680291	-1.346955
C	-0.933468	-3.177633	-1.397252
H	3.659393	-2.871332	-1.851305
C	1.508138	-3.406801	-1.836451
H	-0.920589	-4.195116	-1.787952
H	-1.542856	-2.555257	-2.056265
H	-1.363936	-3.191902	-0.394898

C2 complex

S_0 min (B3LYP/6-31+G(d,p)

Fe	0.908138	0.516471	-0.309459
C	0.532869	1.605321	-2.926955
C	-0.193443	2.061259	-4.029350
N	-0.096575	1.150955	-1.831930
N	-1.532158	2.054287	-4.006718
C	-1.438231	1.149702	-1.814867
C	-2.166178	1.606460	-2.916024
N	1.911593	1.542063	-2.766089
C	2.391079	1.034431	-1.562203
C	2.943667	1.929216	-3.619515
N	3.732101	1.116487	-1.705981
C	4.085196	1.657916	-2.947463
N	-1.916388	0.658143	-0.606214
C	-3.221522	0.506207	-0.140197
C	-0.974379	0.269850	0.341784
C	-3.099534	0.014671	1.113585
N	-1.734098	-0.121084	1.388635
C	-1.243828	-0.639076	2.674772
C	4.741677	0.679139	-0.729857
C	2.279691	0.722459	2.191027
C	3.004699	0.263496	3.292832
N	1.912148	-0.120065	1.212707
N	3.341680	-1.028875	3.389301
C	2.257051	-1.412874	1.313385
C	2.978686	-1.874548	2.417123
N	1.842803	2.013499	1.920927
C	1.126493	2.212378	0.744440
C	2.011380	3.196959	2.637837
N	0.861942	3.537326	0.765177
C	1.392031	4.150559	1.906299
N	1.804138	-2.132139	0.214036
C	1.955331	-3.478477	-0.114834
C	1.098536	-1.432014	-0.760188
C	1.333951	-3.628589	-1.306160
N	0.821071	-2.381455	-1.681311
C	0.057509	-2.195664	-2.924917

C	0.095368	4.288344	-0.240839
H	0.295880	2.430622	-4.923355
H	-3.250211	1.612022	-2.922602
H	2.779790	2.353537	-4.596315
H	5.114256	1.805978	-3.234013
H	-4.093442	0.758499	-0.720830
H	-3.855541	-0.244138	1.837610
H	3.312078	0.928171	4.092185
H	3.263431	-2.915326	2.520445
H	2.544169	3.254660	3.572616
H	1.284959	5.207860	2.088718
H	2.479621	-4.187538	0.504328
H	1.217034	-4.504295	-1.924637
C	-1.461850	-2.147840	2.832872
H	-1.761035	-0.089489	3.467201
H	-0.186412	-0.389876	2.738138
C	-0.955380	-2.655320	4.189683
H	-0.946747	-2.672894	2.019082
H	-2.530507	-2.374877	2.731268
C	-1.156626	-4.164591	4.379728
H	-1.473209	-2.116088	4.995164
H	0.112298	-2.415618	4.292652
C	-0.654889	-4.680267	5.735059
H	-0.639113	-4.703924	3.573359
H	-2.224568	-4.403953	4.274572
C	-0.856983	-6.188745	5.919375
H	-1.918385	-6.456276	5.853081
H	-0.488953	-6.524333	6.895072
H	-0.322733	-6.756267	5.147925
H	-1.172857	-4.141016	6.540119
H	0.411800	-4.438698	5.840675
C	5.471986	-0.594921	-1.169150
H	4.227903	0.528290	0.217555
H	5.448802	1.503575	-0.596025
C	6.521118	-1.037331	-0.140652
H	5.958866	-0.419215	-2.136526
H	4.736649	-1.394041	-1.324688
C	7.282386	-2.299797	-0.566619
H	6.030457	-1.217670	0.825927
H	7.237635	-0.220153	0.022531
C	8.334563	-2.751412	0.454910
H	7.772439	-2.117904	-1.533894
H	6.565740	-3.116871	-0.733263
C	9.093608	-4.011327	0.022693
H	9.622107	-3.848830	-0.924320
H	8.408875	-4.855968	-0.119963
H	9.835887	-4.306779	0.772219
H	7.844684	-2.933160	1.421495
H	9.049099	-1.933639	0.621988
C	-1.354119	-2.789304	-2.849226
H	0.629071	-2.664397	-3.731744
H	0.023388	-1.126893	-3.126819
C	-2.120859	-2.608363	-4.166049
H	-1.902391	-2.313286	-2.026937
H	-1.286882	-3.857618	-2.608623
C	-3.532558	-3.208680	-4.125382
H	-1.552829	-3.073372	-4.983886
H	-2.188631	-1.537905	-4.404714
C	-4.306174	-3.036194	-5.439256
H	-4.101230	-2.744114	-3.306992
H	-3.464085	-4.279147	-3.883989
C	-5.715252	-3.638519	-5.393623
H	-5.678351	-4.714985	-5.187713
H	-6.239799	-3.498885	-6.345146
H	-6.319909	-3.170665	-4.607395
H	-3.736749	-3.500119	-6.256406
H	-4.373502	-1.966441	-5.680883
C	-1.280383	4.728531	0.272105
H	-0.002524	3.646248	-1.113874
H	0.695088	5.156069	-0.532937

C	-2.065199	5.503102	-0.794789
H	-1.153970	5.357020	1.162531
H	-1.846177	3.842543	0.585923
C	-3.441180	5.972544	-0.303934
H	-2.192879	4.869561	-1.683570
H	-1.478448	6.374831	-1.116715
C	-4.235325	6.747099	-1.364040
H	-3.311501	6.606175	0.585165
H	-4.026950	5.100955	0.021846
C	-5.607634	7.216014	-0.866767
H	-6.230136	6.365474	-0.563947
H	-6.148396	7.764349	-1.645833
H	-5.507913	7.879729	0.000458
H	-4.365136	6.113507	-2.252297
H	-3.648242	7.616602	-1.690420

C3 complex

S_0 min (B3LYP/6-31+G(d,p)

Fe	0.139596	0.097190	-0.089420
C	-0.394636	1.403141	-2.586129
C	-1.188478	1.965851	-3.585465
N	-0.948840	0.910907	-1.466377
C	-2.561478	1.979618	-3.337379
C	-2.283316	0.978063	-1.338338
N	-3.129247	1.489391	-2.215601
N	0.982590	1.252242	-2.547435
C	1.523222	0.639946	-1.415352
C	1.969216	1.613815	-3.465696
N	2.848450	0.644502	-1.667071
C	3.138304	1.226502	-2.907098
N	-2.681699	0.422989	-0.127316
C	-3.950673	0.298402	0.433753
C	-1.688682	-0.097438	0.693816
C	-3.752614	-0.309525	1.626696
N	-2.378379	-0.543675	1.765114
C	-1.785017	-1.163672	2.952335
C	3.876292	0.075277	-0.792910
C	1.710484	-0.038795	2.303239
N	2.457215	-0.502837	3.290234
N	1.223171	-0.747047	1.273155
C	2.736857	-1.821040	3.223279
C	1.509973	-2.057412	1.215930
C	2.289413	-2.660480	2.202843
N	1.326649	1.293286	2.201406
C	0.545242	1.655815	1.108723
C	1.603743	2.373802	3.035672
N	0.354772	2.978513	1.297252
C	0.988486	3.432947	2.461393
N	0.929461	-2.628593	0.094034
C	0.954944	-3.939646	-0.383031
C	0.175154	-1.789577	-0.726784
C	0.209327	-3.925238	-1.511076
N	-0.256679	-2.618681	-1.700341
C	-1.086997	-2.223470	-2.840859
C	-0.417675	3.867645	0.430372
H	-0.776983	2.370261	-4.500611
H	-3.241153	2.402596	-4.070053
H	1.757637	2.105057	-4.401079
H	4.149630	1.314638	-3.271027
H	-4.842998	0.644266	-0.060742
H	-4.457443	-0.599531	2.389612
H	-1.233029	-0.421566	3.532475
H	-2.586092	-1.570622	3.568351
H	-1.121775	-1.976336	2.657765
H	4.838888	0.514712	-1.053050
H	3.648667	0.315852	0.243765
H	3.928379	-1.008104	-0.921825
H	3.348395	-2.220568	4.025847
H	2.538186	-3.713244	2.189440

H	2.197070	2.281222	3.930080
H	0.940520	4.466405	2.766504
H	1.482118	-4.740528	0.108360
H	-0.036658	-4.721851	-2.195059
H	-0.501554	-1.642054	-3.555873
H	-1.454676	-3.123807	-3.331644
H	-1.939877	-1.641566	-2.493994
H	0.208845	4.702088	0.109139
H	-0.748621	3.310460	-0.440318
H	-1.286815	4.250351	0.970002

$S_0/^3MC$ singlet-triplet crossing (TD-HCTH/6-31G*)

Fe	0.290203	-0.127798	0.055733
C	-0.619386	1.538865	-2.824439
C	-1.305876	2.521632	-3.541727
N	-1.277409	0.759895	-1.992600
C	-2.657126	2.659673	-3.194895
C	-2.471342	1.121673	-1.587497
N	-3.252081	2.027609	-2.164070
N	0.756690	1.294756	-2.729777
C	1.283989	0.701368	-1.575698
C	1.748383	1.663418	-3.622850
N	2.616829	0.719378	-1.825368
C	2.916174	1.289270	-3.054260
N	-2.780025	0.512936	-0.359814
C	-4.025102	0.412569	0.232699
C	-1.763238	0.018691	0.457904
C	-3.814091	-0.174196	1.432585
N	-2.449647	-0.399998	1.550648
C	-1.858246	-0.999495	2.738671
C	3.645784	0.226002	-0.920337
C	1.846214	-0.170756	2.469551
N	2.581645	-0.596627	3.481664
N	1.369034	-0.914529	1.455609
C	2.854345	-1.911026	3.454852
C	1.655652	-2.228956	1.444504
C	2.418072	-2.792706	2.456908
N	1.447687	1.138545	2.298043
C	0.670264	1.413916	1.169206
C	1.689606	2.265142	3.064645
N	0.453599	2.749474	1.282186
C	1.060526	3.273481	2.417847
N	1.086428	-2.825955	0.327091
C	1.127830	-4.134621	-0.111835
C	0.347961	-2.007268	-0.527898
C	0.405948	-4.152146	-1.260175
N	-0.055030	-2.867309	-1.493026
C	-0.859570	-2.511253	-2.654190
C	-0.311465	3.560570	0.350624
H	-0.846787	3.171128	-4.278157
H	-3.275743	3.377743	-3.729911
H	1.536926	2.123472	-4.576113
H	3.930339	1.372221	-3.416057
H	-4.924744	0.751282	-0.257047
H	-4.509687	-0.454147	2.209842
H	-1.147358	-0.309652	3.197174
H	-2.652134	-1.210035	3.455193
H	-1.358340	-1.936639	2.485491
H	4.621917	0.394714	-1.375077
H	3.603251	0.763921	0.028701
H	3.519399	-0.844837	-0.748060
H	3.457751	-2.289210	4.277470
H	2.669819	-3.845937	2.488436
H	2.272550	2.237629	3.971830
H	0.990004	4.322390	2.665705
H	1.648881	-4.923219	0.408907
H	0.182919	-4.971136	-1.927878
H	-0.298184	-1.838296	-3.305525
H	-1.104769	-3.421826	-3.200876
H	-1.779274	-2.022973	-2.332115

H	-0.300081	4.594806	0.695022
H	0.136033	3.518387	-0.644368
H	-1.347102	3.216840	0.308527

C4 complex

S_0 min (B3LYP/6-31+G(d,p)

Fe	0.830195	0.438790	-0.272198
C	0.346681	1.415589	-2.911293
C	-0.436222	1.811642	-4.000786
N	-0.239315	1.047935	-1.757762
N	-1.769285	1.831562	-3.903898
C	-1.579348	1.077073	-1.660641
C	-2.353686	1.473689	-2.756810
N	1.731096	1.324325	-2.821038
C	2.252035	0.849860	-1.612060
C	2.754966	1.649081	-3.729529
N	3.589297	0.869867	-1.776301
C	3.944167	1.352947	-3.048354
N	-2.000369	0.672585	-0.398621
C	-3.278320	0.600020	0.184794
C	-1.002598	0.288697	0.505661
C	-3.049580	0.145640	1.491082
N	-1.662094	-0.032580	1.636027
C	-1.062029	-0.525019	2.885961
C	4.594190	0.427478	-0.796908
C	2.343131	0.674592	2.137463
C	3.095301	0.210698	3.221760
N	1.893924	-0.189244	1.209510
N	3.380476	-1.089924	3.340636
C	2.184703	-1.495725	1.330394
C	2.942429	-1.949053	2.416034
N	1.954621	1.976178	1.840506
C	1.179734	2.155789	0.688309
C	2.231310	3.203065	2.470536
N	0.967599	3.484838	0.614652
C	1.594122	4.165024	1.674626
N	1.644190	-2.230457	0.280763
C	1.709512	-3.599553	-0.036292
C	0.907387	-1.518713	-0.673350
C	0.981625	-3.725478	-1.227632
N	0.513542	-2.444311	-1.570422
C	-0.320244	-2.210166	-2.760179
C	0.186933	4.192435	-0.410611
H	-0.005065	2.105322	-4.946998
H	-3.433517	1.499955	-2.723905
H	3.466035	0.869318	3.993869
H	3.195191	-2.990909	2.550886
C	-1.263769	-2.027143	3.093672
H	-1.505871	0.046533	3.705921
H	-0.006088	-0.273225	2.854235
H	-0.807384	-2.604240	2.285114
H	-2.323183	-2.290517	3.146369
C	5.149039	-0.965096	-1.101509
H	4.123663	0.457208	0.181741
H	5.392582	1.174230	-0.793264
H	5.639707	-0.999136	-2.077760
H	4.357746	-1.719390	-1.089865
C	-1.769215	-2.663062	-2.570615
H	0.149271	-2.739515	-3.593952
H	-0.267789	-1.148891	-2.985026
H	-2.248240	-2.127744	-1.746467
H	-1.834516	-3.734714	-2.366017
C	-1.196200	4.638458	0.082162
H	0.097605	3.529466	-1.267502
H	0.779179	5.055520	-0.730488
C	-1.944186	5.427814	-0.997720
H	-1.086169	5.254510	0.980978
H	-1.776335	3.757282	0.376679
H	-2.087339	4.828508	-1.903533

H	-1.396748	6.334913	-1.276968
C	5.194946	1.564402	-3.625893
C	5.217910	2.082588	-4.922049
C	4.028504	2.377467	-5.607758
C	2.775927	2.168773	-5.024723
H	6.114575	1.341105	-3.097897
H	6.172558	2.260768	-5.405681
H	4.077125	2.780157	-6.613957
H	1.878505	2.413171	-5.575869
C	-4.568171	0.886881	-0.264533
C	-4.091654	-0.035594	2.398869
C	-5.382941	0.249522	1.951184
C	-5.615004	0.701174	0.642018
H	-6.629256	0.915314	0.321979
H	-6.220304	0.119842	2.628673
H	-4.776985	1.243955	-1.263285
H	-3.915749	-0.381009	3.410695
C	2.957236	3.570927	3.604535
C	1.661304	5.525569	1.970379
C	2.387053	5.895628	3.104062
C	3.020884	4.933547	3.906780
H	1.175789	6.270766	1.351346
H	2.461407	6.945438	3.367446
H	3.577420	5.250144	4.782557
H	3.461501	2.855503	4.238855
C	2.315916	-4.706458	0.559590
C	0.835297	-4.952101	-1.873304
C	2.166647	-5.938047	-0.083122
C	1.441714	-6.060517	-1.279448
H	2.626377	-6.817055	0.356117
H	2.885276	-4.643340	1.476320
H	0.277481	-5.050146	-2.797047
H	1.349668	-7.032610	-1.752248
H	-0.794441	-2.322635	4.036460
H	5.889182	-1.229111	-0.340609
H	-2.329394	-2.458608	-3.487619
H	-2.931611	5.730631	-0.637058

$S_0/^3$MC singlet-triplet crossing (TD-HCTH/6-31G*)

Fe	0.972381	0.364521	-0.017931
C	0.196157	1.425613	-3.207746
C	-0.528100	1.298198	-4.403225
N	-0.459313	1.455668	-2.069315
N	-1.854916	1.137861	-4.353063
C	-1.730614	1.133614	-1.989086
C	-2.473900	1.012790	-3.174453
N	1.581380	1.382695	-2.986016
C	2.084420	0.844957	-1.793388
C	2.603829	1.772523	-3.849036
N	3.429078	0.888129	-1.958665
C	3.791999	1.452611	-3.183632
N	-2.083892	0.815133	-0.668306
C	-3.350268	0.838459	-0.085472
C	-1.111426	0.341109	0.225740
C	-3.172590	0.340338	1.209816
N	-1.814607	0.044399	1.346369
C	-1.282119	-0.576254	2.561826
C	4.433811	0.362268	-1.031117
C	2.500323	0.629352	2.380880
C	3.223830	0.171602	3.478730
N	2.062866	-0.247846	1.452627
N	3.514951	-1.128423	3.616805
C	2.363513	-1.555226	1.585289
C	3.105759	-1.990566	2.690882
N	2.111695	1.927230	2.057266
C	1.306843	2.085323	0.927213
C	2.411418	3.155349	2.650078
N	1.088174	3.416221	0.843374
C	1.744675	4.106791	1.860495
N	1.828069	-2.271971	0.537961

C	1.902795	-3.624438	0.190651
C	1.058256	-1.536786	-0.385524
C	1.140788	-3.735582	-0.981286
N	0.645849	-2.465395	-1.284069
C	-0.236812	-2.227743	-2.423047
C	0.241672	4.090628	-0.141647
H	-0.065236	1.279583	-5.385202
H	-3.533471	0.776721	-3.196595
H	3.568141	0.830274	4.265667
H	3.361061	-3.032140	2.844123
C	-1.582596	-2.066825	2.656210
H	-1.705280	-0.035711	3.413997
H	-0.210765	-0.394337	2.577088
H	-1.165116	-2.611175	1.803679
H	-2.657103	-2.266379	2.697033
C	4.995429	-0.990020	-1.451418
H	3.970300	0.301583	-0.050790
H	5.229173	1.110451	-0.957624
H	5.515197	-0.937760	-2.412196
H	4.206089	-1.743435	-1.530331
C	-1.658251	-2.735728	-2.209088
H	0.219619	-2.702596	-3.297926
H	-0.227778	-1.158241	-2.606234
H	-2.117468	-2.279857	-1.327021
H	-1.691649	-3.821511	-2.085851
C	-1.121390	4.507325	0.418262
H	0.122895	3.404719	-0.976527
H	0.796356	4.962604	-0.503627
C	-1.981633	5.191744	-0.639003
H	-0.983821	5.179715	1.272710
H	-1.636182	3.618935	0.803220
H	-2.181805	4.529956	-1.490099
H	-1.499178	6.097448	-1.025031
C	5.038668	1.735970	-3.741977
C	5.048529	2.355183	-4.988946
C	3.855973	2.691216	-5.647695
C	2.611397	2.412865	-5.088093
H	5.966055	1.496581	-3.232451
H	6.001614	2.590357	-5.455130
H	3.899551	3.187653	-6.613408
H	1.699604	2.705679	-5.596366
C	-4.592144	1.293075	-0.528358
C	-4.236813	0.248940	2.107067
C	-5.482493	0.680559	1.658873
C	-5.655512	1.197763	0.366139
H	-6.638100	1.541111	0.053806
H	-6.334839	0.623870	2.330629
H	-4.735695	1.723677	-1.512899
H	-4.109707	-0.131824	3.114936
C	3.189119	3.547766	3.739885
C	1.828061	5.473299	2.129670
C	2.599030	5.860187	3.220322
C	3.266622	4.912068	4.009825
H	1.320614	6.209484	1.515646
H	2.687706	6.916144	3.460506
H	3.866389	5.244543	4.852696
H	3.731405	2.846962	4.360815
C	2.553802	-4.729795	0.735756
C	1.005312	-4.952104	-1.648202
C	2.410873	-5.947555	0.071996
C	1.651726	-6.057613	-1.099723
H	2.907264	-6.825806	0.475722
H	3.160656	-4.673240	1.630298
H	0.426827	-5.044039	-2.561123
H	1.565649	-7.020870	-1.595420
H	-1.130498	-2.462248	3.571556
H	5.714540	-1.324276	-0.696560
H	-2.262971	-2.478535	-3.084808
H	-2.946552	5.485131	-0.212556

Transient absorption spectroscopy

Additional data and fit results for the four complexes

Data analysis

For **C1** and **C3,** the single kinetic traces are fitted by the equation (1)

$$F(t) = \left[\sum_{i=1}^{n} a_i e^{-t/\tau_i}\right] \otimes IRF\,(t_0, \sigma) \qquad (1)$$

Where n is the number of the kinetic species, a_i is the amplitude associated to the decay time τ_i. After visual inspection of the kinetic traces on a semi-log scale, 3 different time scales are identified and, n=3 is used for all wavelengths. The sum is convoluted with the Instrument Response Function (IRF) that is assumed to have a Gaussian shape with 50 fs FWHM. The time zero position t_0 is fitted, but constrained to be within ± 100 fs (tolerance of chirp correction). Fits are performed using the ORIGIN software.

The quality of the fit is evaluated by visual inspection, as exemplified by figure SI22. The shape of the residuals, ideally statistically distributed around zero and the agreement with the long time decay slope are the main criteria for tuning fit parameters (e.g. three instead of two decay fits).

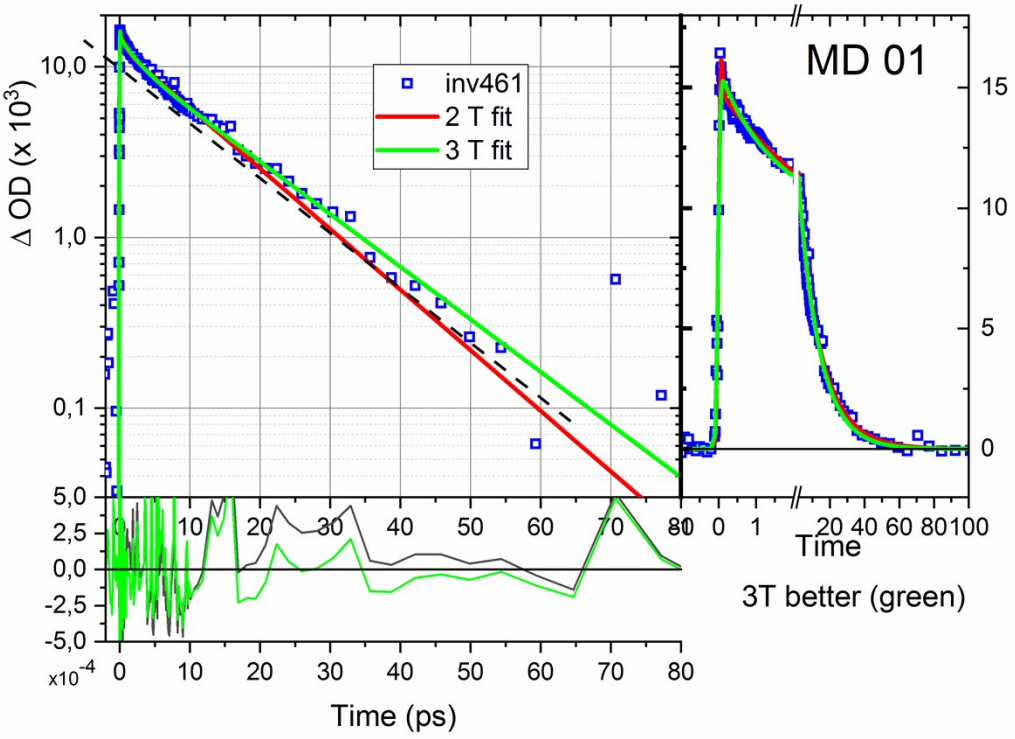

Figure SI22: Example of fit quality evaluation by visual inspection. The top panels show the agreement between data (open symbols) and fit curves (solid lines). Bottom left panel: residuals. The example shows that a 3-time is better than with two time components only.

Analysis of the spectra and kinetics of C4

In Fig SI23 the spectra reported in Fig 4A are shown normalized at 473 nm. The SSA is normalized at the same wavelength, sign-inverted and added into the graph for comparison (pink dash-dot line). In the case of a single photo-induced species, all wavelengths decay with the same time constant, and the normalized spectra should perfectly overlay for all time points. Deviations are then due to the contribution of additional species or to a time-dependence of the extinction coefficient of the photo-excited species (e.g. due to vibrational or dielectric relaxation).
As discussed in the main text, for **C4**, three signals are present, two positives (ESA) and one negative (GSB). The isosbestic point at 428 and 500 nm are preserved after the normalization for the spectra at t>1 ps. The 0.1 and 0.2 ps spectra show small differences in the ESA at λ< 428 nm while in the other ESA the differences are more pronounced.

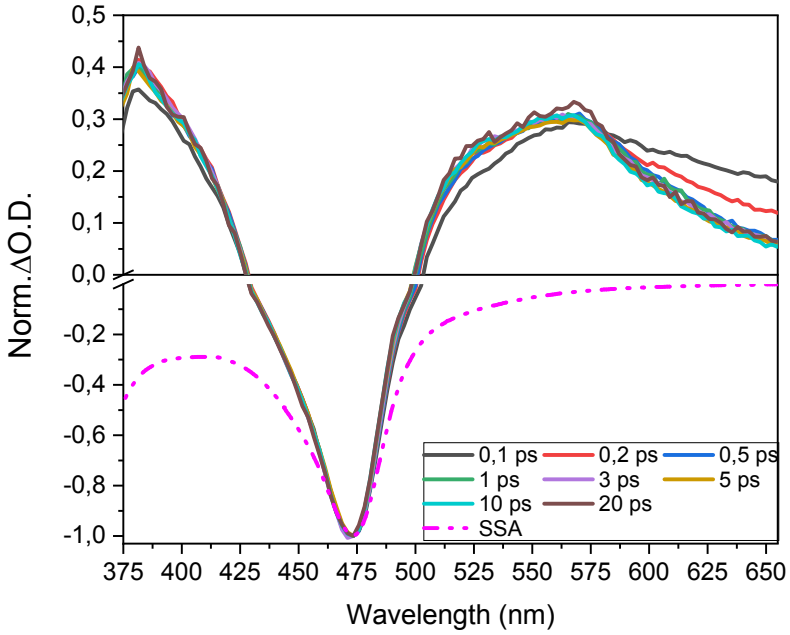

Figure SI23 Selected spectra of C4 normalized at 473 nm. The inverse of steady-state absorption (pink dot-dash line) is shown for comparison

To emphasize these differences, in Fig SI24, the normalized 20 ps spectrum is subtracted from the other normalized spectra. Only the spectra until 1 ps are reported because at longer times no change in the norm. spectra is observed. Three zones can be identified: λ> 590 nm, 590-490 nm and < 460 nm. In the first region, the intensity of the ESA band decays 50% in 100 fs and completely in 0.5 ps. In the second region, in the same time-scale the ESA rises and gets the final shape. In the third zone, the same trend is observed but the low signal/noise ration prevents a more detailed investigation.

In conclusion, for this sample, the spectral evolution within the first 0.5 ps is attributed to the 1MLCT→ 3 MLCT transition, and vibrational relaxation within ^{3}MLCT. It is represented by the τ_1 component obtained from global fitting.

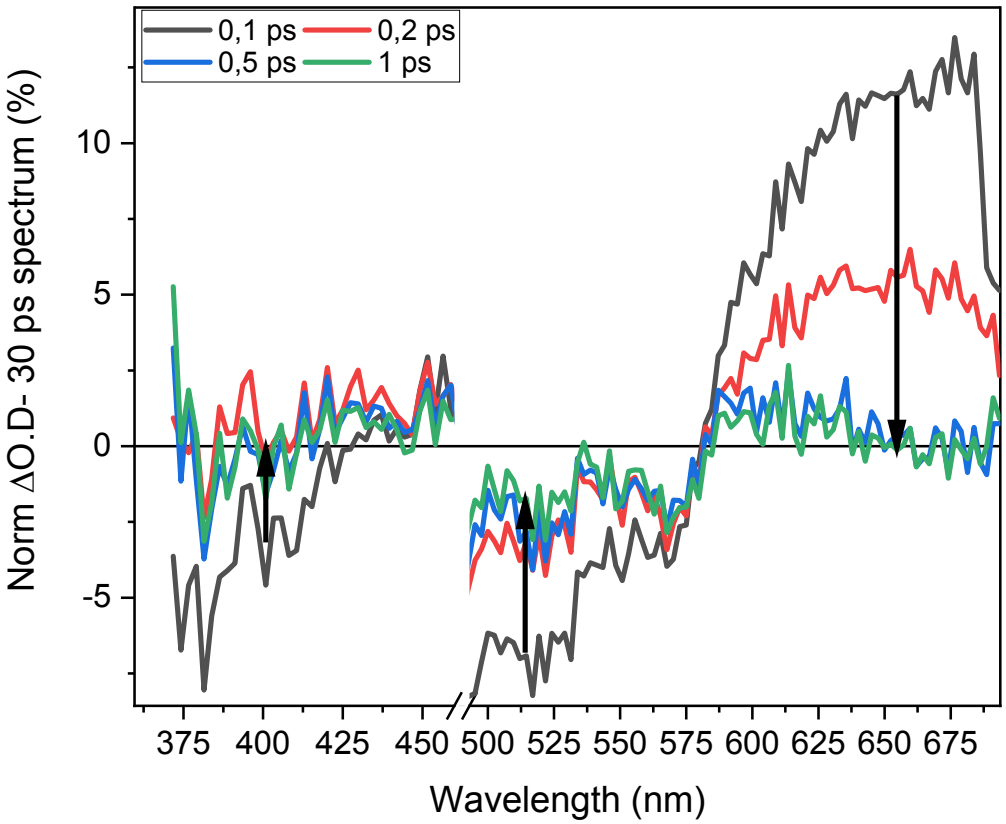

Figure SI24: Double difference spectra, computed from the normalized spectra in figure SI23, by subtraction of the normalized 20 ps spectrum. These spectra highlight the spectral changes during the first 1.0 ps, related to the ^{1}MLCT-^{3}MLCT transition.

Analysis of the spectra and kinetics of C2

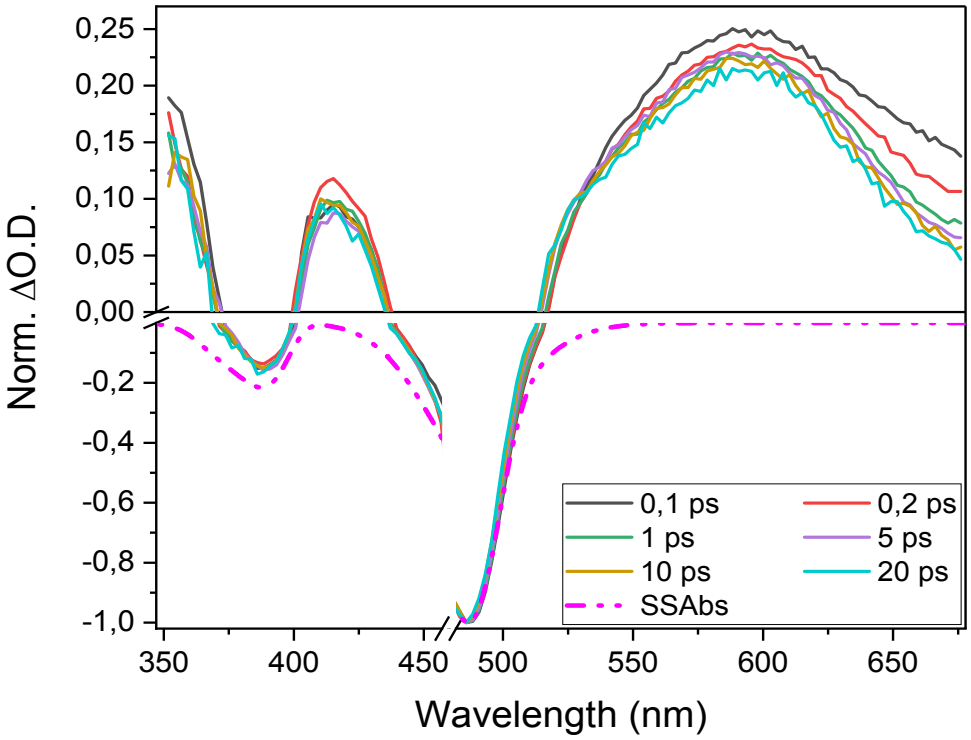

Figure SI25: Selected spectra of C2 normalized at 486 nm. The inverse of steady-state absorption (pink dot-dash line) is shown for comparison

The same analysis was performed for **C2;** the spectra reported in Fig 3B are normalized at 486 nm together with the sign-inverted SSA (Fig SI25). After the normalization, the negative signals are fully overlapping, while the positive ones show a time evolution. The main contribution develops at λ> 530 nm, but also below this wavelength, where the curves do not overlap at any time. While the signal decays at longer wavelengths, it rises in the range of 500-530 nm, leading to a small 3 nm shift of the ESA/GSB crossover point.

This evolution is better highlightes in Fig SI26. As before the normalized 20 ps spectrum is subtracted from the others. The low signal/noise ratio prevents the investigation of the region at λ<450 nm while the others can be separated in 3 parts: λ> 617 nm, 617<λ<530 nm and 529<λ<490 nm. Differently from **C4**, in the first and second region, the double difference does not vanish in 0.5 ps but the evolution extends up to ≈ 10 ps. In the third zone, the signal increase is limited to a sharp a 30 nm broad region, limited on the lower wavelength side by the normalization point (486 nm). This rising high-energy ESA edge precludes the maintenance of the isosbestic point at 516 nm.

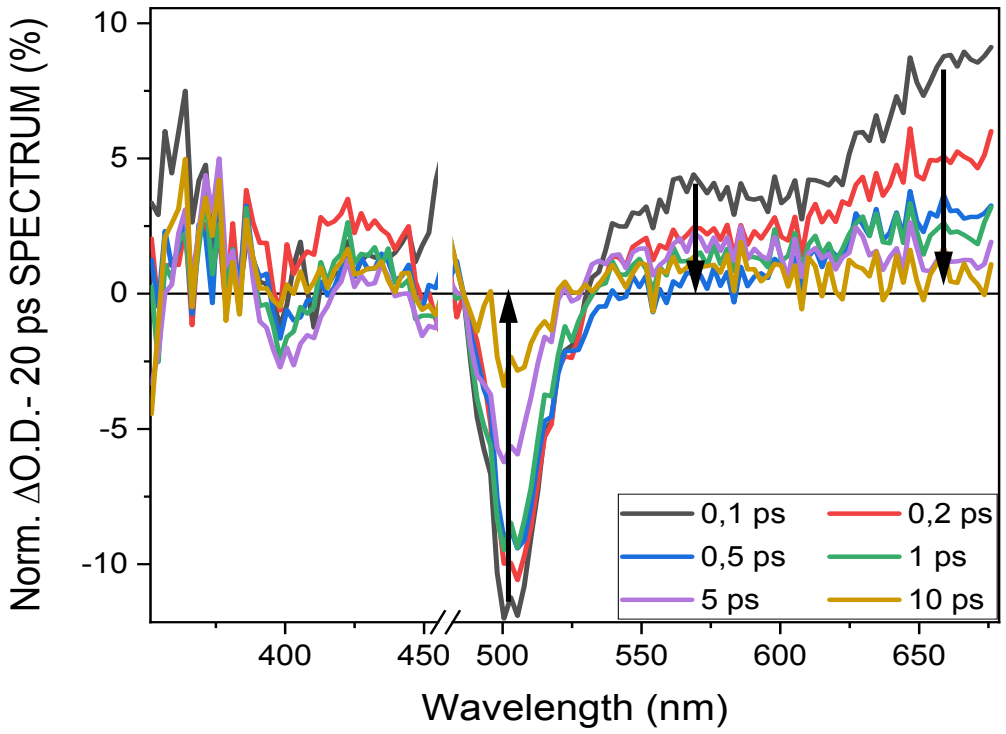

Figure SI26: Double difference spectra, computed from the normalized spectra in figure SI25, by subtraction of the normalized 20 ps spectrum. These spectra highlight the spectral changes during the first 10 ps, related to the ^{1}MLCT-^{3}MLCT transition, and a small blue-shift of the ESA spectrum at longer times (rise in the 490-530 nm range).

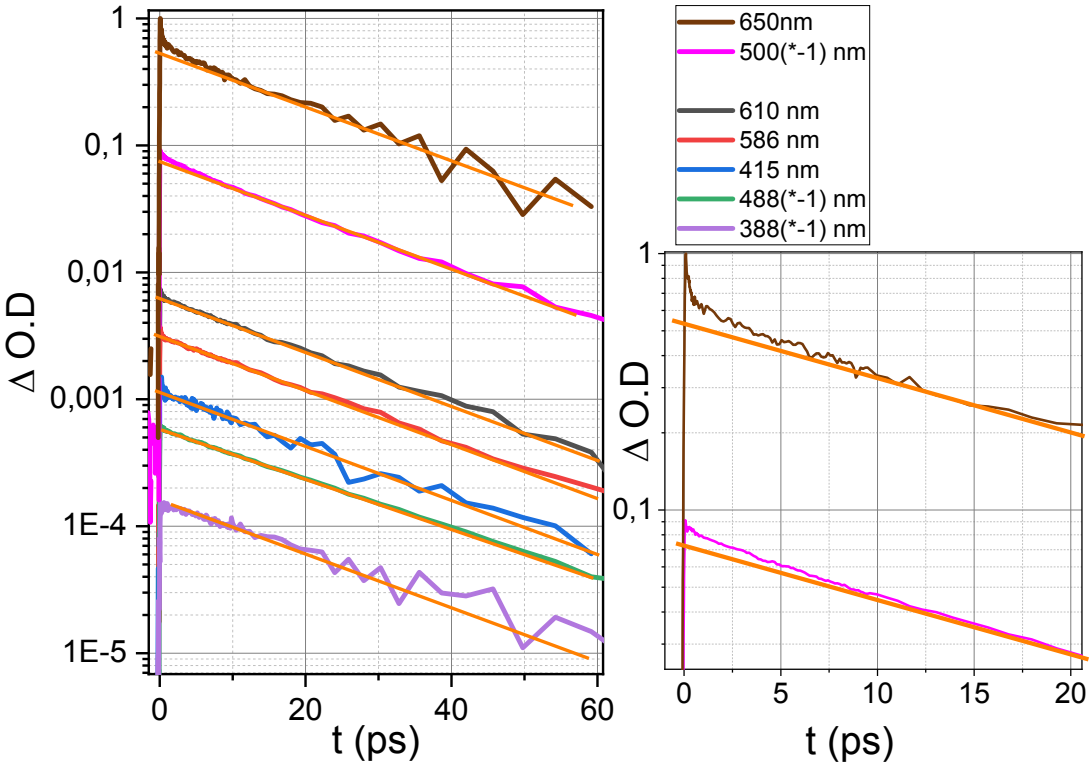

Figure SI27: Selected kinetic traces of **C2,** normalized and multiplied by an arbitrary factor for vertical displacement on the log. intensity scale. GSB kinetic traces are sign-inverted. Left: Selected wavelengths cover the main and secondary bleach band (488 and 388 nm), the main and secondary ESA (610, 586 and 415 nm). Right: A zoom into the first 20 ps of the long wavelength ESA decay (650 nm), and GSB close to the ESA/GSB crossover (500 nm). A small amplitude 2-3 ps lifetime is visible, which is associated with the ESA blue-shift displayed in figs. SI26 and SI25.

The major part of the kinetic traces of **C2** decay with a ≈20ps time constant (left). A zoom into the 650 nm ESA trace (right) shows a sub-ps component, associated with the 1MLCT-3MLCT relaxation, plus a small amplitude 2-3 ps lifetime associated with the ESA blue-shift.

Analysis of the spectra and kinetics of **C1**

The normalized spectra of **C1** are reported in Fig SI28. The normalization is done at the ESA maximum at ≈580 nm. This compound presents a more pronounced time evolution than the previous ones. The SSA is overlapping with the normalized transient absorption spectra in a modest region (445-493nm) because an important ESA band reduces the GSB for shorter wavelengths. The curves in the minor GSB are approximately overlapping after 0.1 ps while both ESA exhibit a reshaping during time, i.e. an increase of intensity on the short wavelength sides. Also for this sample, to emphasize the differences, the 20 ps spectrum is subtracted from the others and the results are plotted in Fig SI29. Two rising bands are underlined in the graph: one peaked at 502 nm and the second at 400 nm.

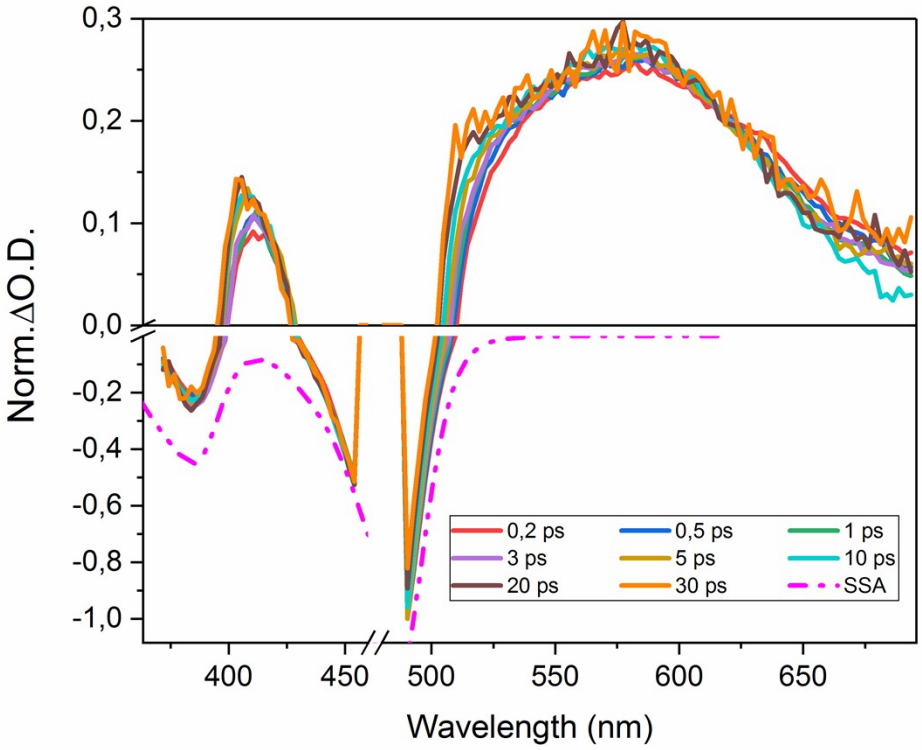

Figure SI28: TAS spectra of **C1**, normalized at the ESA maximum at 580 nm.

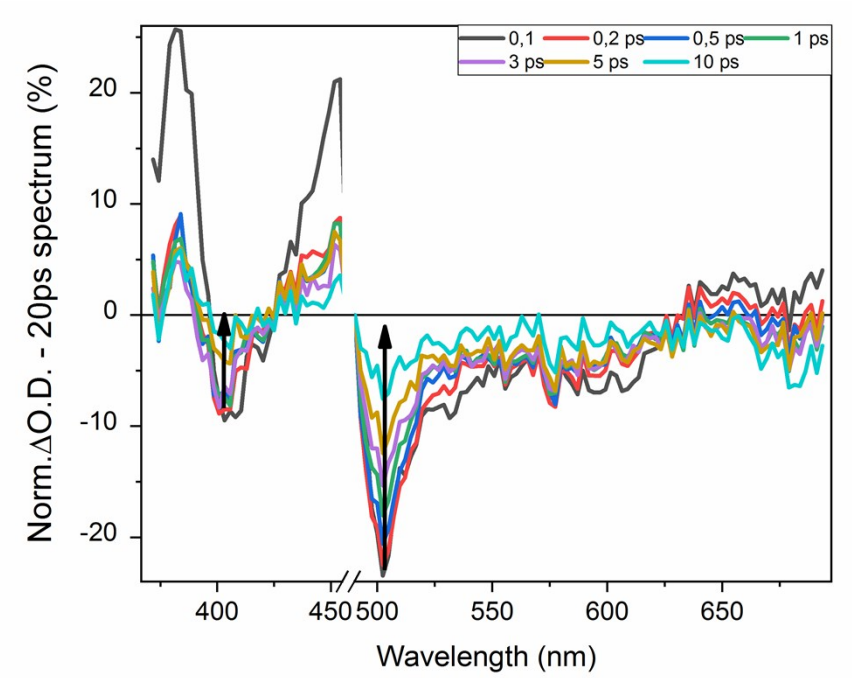

Figure SI29: Double difference spectra: Normalised spectra of Fig. SI28, after subtraction by the norm. 20 ps spectrum. The progressive signal increase in the 400-410 and 490-620 nm underscores the spectral blue-shift of the ESA transitions.

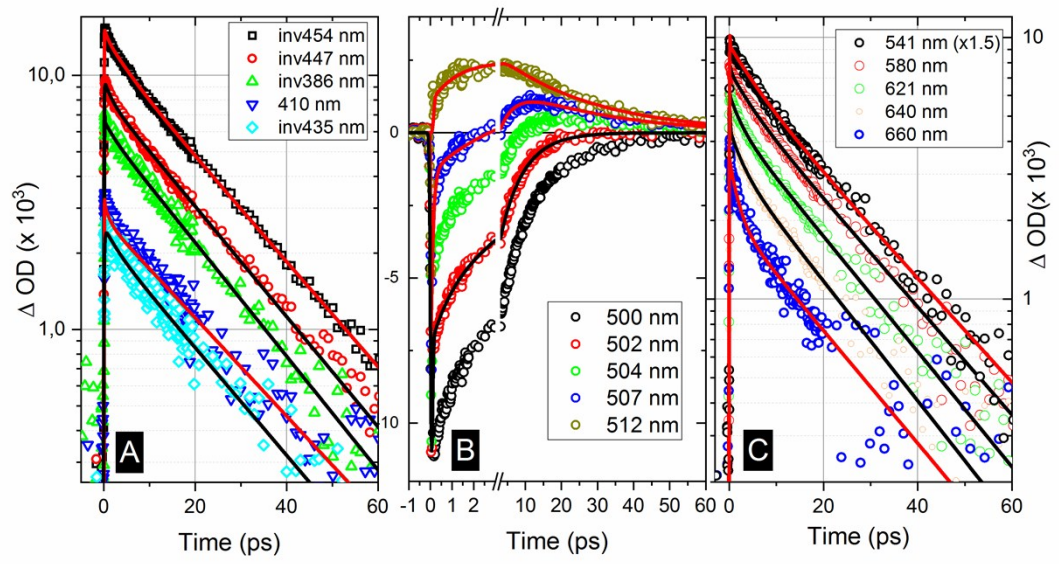

Figure SI30: Kinetic traces of **C1**. A: GSB bleach traces are sign-inverted; B: Crossover region; C: ESA wavelength, 541 nm trace vertically shifted. The semi-log plot gives evidence for the three lifetimes / components used in the fits. The ESA region displays a strongly wavelength-dependent decay consistent with the ESA blue-shift. Fit results are reported in figure 7, main text.

The ESA blue-shifts are also reflected in the kinetic traces of C1 displayed in Figure SI30 for the three separate regions: GSB (λ <454), the ESA/GSB crossover region (490-520nm), and main ESA band (> 520 nm). The main ESA band displays a strongly wavelength-dependent decay consistent with the ESA blue-shift. Fit results are reported in figure 7, main text. As for **C3** (see below), the crossover region displays an apparent rise time, and a wavelength-dependent time of zero-crossing. The traces are the results of compensating ESA and GSB traces with wavelength-dependent amplitudes. The lifetimes reported in figure 7 for the crossover region were freely fitted (large error bars), and represent the apparent signal properties, not necessarily the relevant molecular time scales.

Analysis of the spectra and kinetics of C3

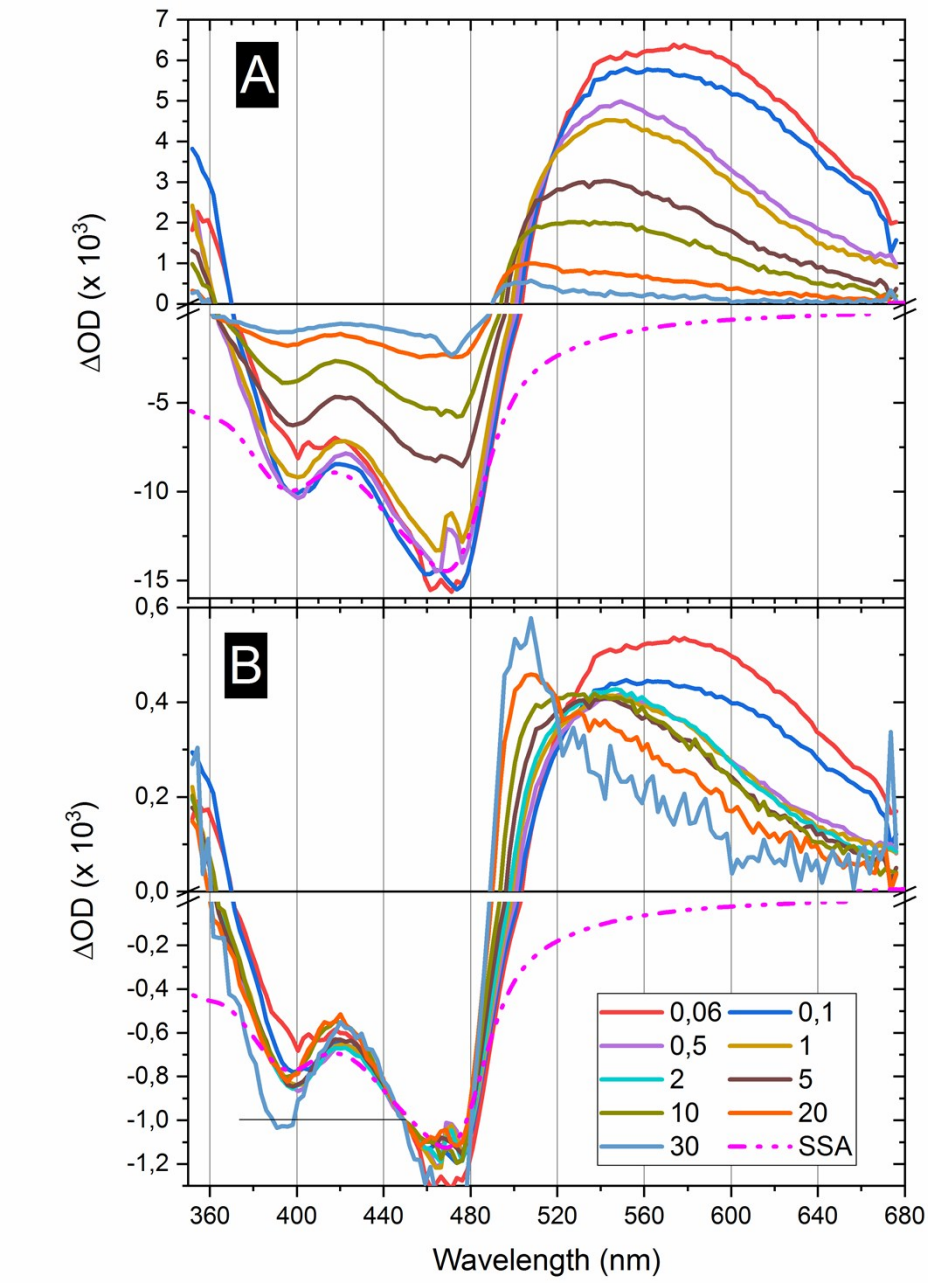

Figure SI31: TAS spectra of C3 for delays up to 30 ps. A: Raw data; B: Normalised at 448 nm. The sign-inverted SSA is scaled and plotted as reference. The spectral relaxation is most prominent in this sample, with a displacement of ≈18 nm of the GSB/ESA crossover wavelength in the first 20 ps.

The time-resolved TAS spectra in Fig SI31 exhibit a broad GSB (380-490 nm) and two ESA bands. The long-wavelength ESA bands displays the most prominent spectral changes among all compounds studied. While the amplitude of ESA and GSB decay overall with an average lifetime of ≈12 ps, the ESA band changes shape and blue-shifts. This is best seen in the normalized ΔOD spectra (Fig. SI31B). The GSB/ESA crossover points shifts by ≈18 nm in the first 20 ps.

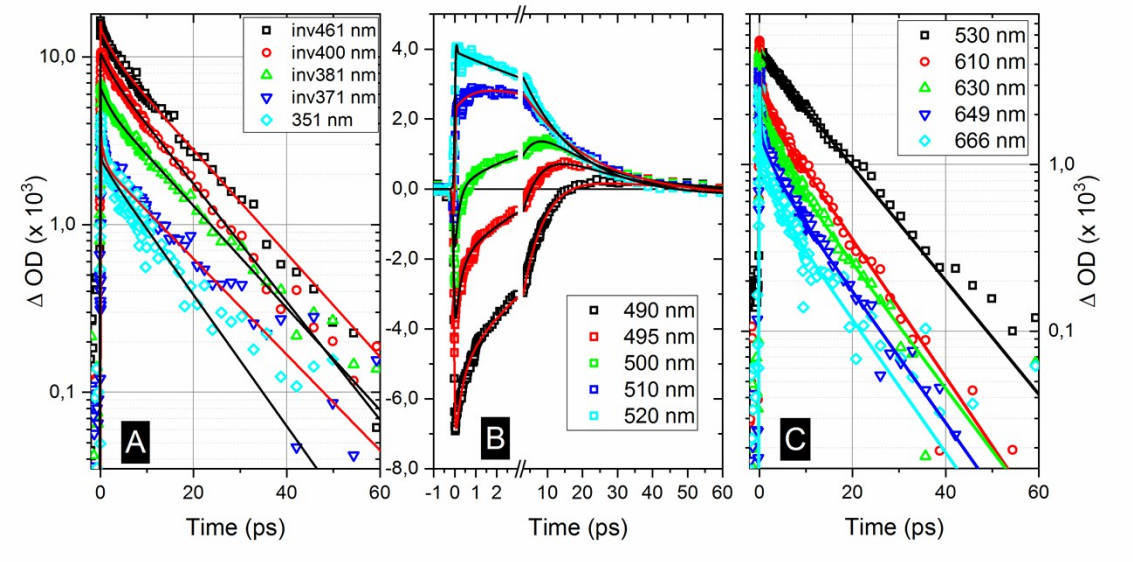

Figure SI32: Representative kinetic traces of C3. A: GSB and blue-ESA (351 nm); B: ESA/GSB crossover region; C: long-wavelength ESA region. The semi-log plot easily identifies the three relevant time scales used for fitting (see Figure SI33). The peculiar shapes of the kinetic traces in the crossover region are due to ESA and GSB traces overlaying and compensating with wavelength-dependent amplitudes.

Visual inspection of the kinetic traces of C3 suggest three relevant time scale used for fitting (see below), with a dominant ≈12 ps identified in both the GSB and ESA (Figs SI32A and SI32C). The ESA seems to display a single wavelength-dependent 8-12 ps lifetime, with the shorter values observed for the longer wavelengths (SI32C), and consistent with the progressive blue-shift and narrowing of the spectra. However, the fit analysis shows that the faster apparent decay is due to two components, τ_2 and τ_3, with wavelength-dependent amplitudes.

The ESA/GSB crossover region is the result of GSB and ESA decaying with very similar lifetimes but wavelength-dependent amplitudes. The kinetics are fitted by a strongly wave-length dependent rise time τ_2 (cf. SI-fitparamsC3), and a lengthening of the τ_3 decay time. However, these are "apparent" lifetimes characterizing the fit. In particular τ_2 the and not should be linked to a molecular process.

The obtained fit results for the three lifetimes and the amplitudes of τ_2 and τ_3, namely A_2 and A_3, are displayed in figure SI33. Lifetimes are relatively constant, and show a strong wavelength dependence only in the GSB/ESA crossover region (green rectangle). The average excited state lifetime of C3 is τ_3 = 11.8±1.0 ps

A_2 is non-zero in the GSB region (370-470 nm) and follows relatively well the scaled SSA. This means that part of the exc. state population decays within τ_2 to the ground state, while spectral relaxation proceeds. Note the large negative A_2 values in the 490-520 nm region, where ESA dominates GSB. A_2 is much larger than the scaled GSB amplitude, indicating that it is clearly a GSB rise and not a ESA decay time in this wavelength region.

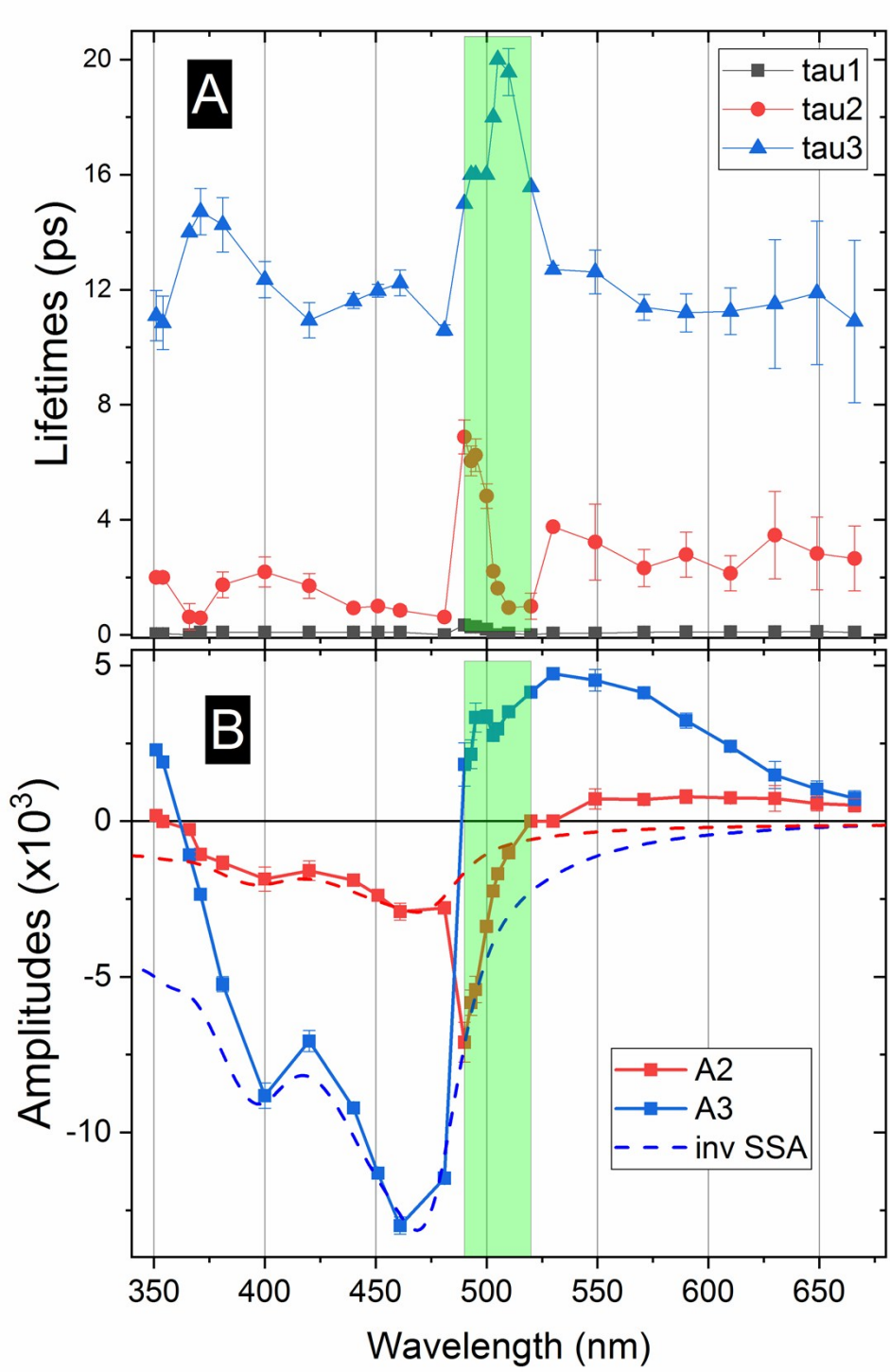

Figure SI33: Results of individual wavelength fits: The three lifetimes and the amplitudes of τ_2 and τ_3, A2 and A3. The green rectangle denotes the ESA/GSB crossover region. Error bars are the fit uncertainties. Zero error bars in τ_3 are due to fixed, non-fitted values (otherwise no convergence).